Environmental Science & Technology

pubs.acs.org/est

Article

Toxicokinetic Models for Bioconcentration of Organic Contaminants in Two Life Stages of White Sturgeon (*Acipenser transmontanus*)

Chelsea Grimard, Annika Mangold-Döring, Hattan Alharbi, Lynn Weber, Natacha Hogan, Paul D. Jones, John P. Giesy, Markus Hecker,* and Markus Brinkmann

Cite This: *Environ. Sci. Technol.* 2021, 55, 11590–11600

Read Online

ACCESS | Metrics & More | Article Recommendations | Supporting Information

ABSTRACT: The white sturgeon (*Acipenser transmontanus*) is an endangered ancient fish species that is known to be particularly sensitive to certain environmental contaminants, partly because of the uptake and subsequent toxicity of lipophilic pollutants prone to bioconcentration as a result of their high lipid content. To better understand the bioconcentration of organic contaminants in this species, toxicokinetic (TK) models were developed for the embryo-larval and subadult life stages. The embryo-larval model was designed as a one-compartment model and validated using whole-body measurements of benzo[*a*]pyrene (B[*a*]P) metabolites from a waterborne exposure to B[*a*]P. A physiologically based TK (PBTK) model was used for the subadult model. The predictive power of the subadult model was validated with an experimental data set of four chemicals. Results showed that the TK models could accurately predict the bioconcentration of organic contaminants for both life stages of white sturgeon within 1 order of magnitude of measured values. These models provide a tool to better understand the impact of environmental contaminants on the health and the survival of endangered white sturgeon populations.

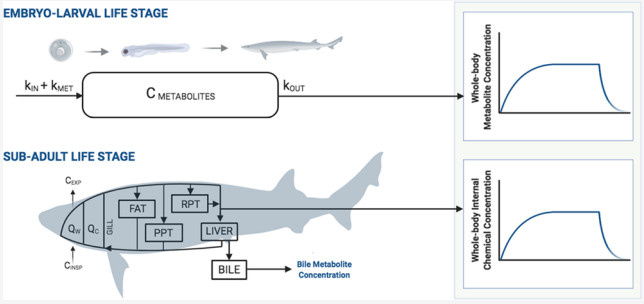

KEYWORDS: *white sturgeon, life-stage extrapolation, B[a]P, organic contaminants, TK models*

1. INTRODUCTION

The white sturgeon (*Acipenser transmontanus*) is an ancient fish species native to the western regions of North America. Presently, as a result of the failure of natural recruitment due in part to degradation of suitable spawning habitat[1−3] and pollution,[4−8] some populations of white sturgeon from northwestern rivers in the United States (U.S.) and British Columbia, Canada, have been classified as endangered.[9−11] Because white sturgeon have been shown to be more sensitive to some contaminants compared to other species, effects of industries on water quality by releases of pollutants could pose chronic threats to wild populations of white sturgeon.[12−15] Therefore, the bioconcentration of contaminants, resulting in adverse effects and ultimately mortality, might be one of the causes hindering successful recruitment in this species.

White sturgeon are unique in their physiology since they have a higher lipid content relative to other freshwater fish.[16] They are bottom dwellers that live near the sediment. As a result of their benthic lifestyle and high lipid content, there is increased potential for exposure and subsequent toxicity to lipophilic contaminants that bioconcentrate from both direct exposure and leaching from sediments.[16] Accordingly, relatively great concentrations of organic contaminants, such as polychlorinated biphenyls, polybrominated diphenyl ethers, polychlorinated dibenzo-*p*-dioxins, polychlorinated dibenzofurans, and organochlorine pesticides, have been reported in wild-caught white sturgeon from northwestern U.S. and Canadian freshwater systems.[4−8] Exposure to polycyclic aromatic hydrocarbons, such as benzo[*a*]pyrene (B[*a*]P), is also a concern since habitats of vulnerable white sturgeon populations overlap with areas that use fossil fuels for industrial processes.[17,18] Previous studies have shown that due to the structure of their aryl hydrocarbon receptors (AhRs) that drive dioxin-like compound (DLC) toxicity,[19] white sturgeon might be more sensitive to adverse effects of DLCs, thus emphasizing the importance of better understanding the bioconcentration of such compounds.

Knowledge of the extent of the bioconcentration of organic contaminants is essential to better understand the effects that pollutants have on the reproductive fitness of white sturgeon. This information, however, can be difficult and often impractical to generate because individual white sturgeon, which are required for restocking programs, necessitates a large

Received: October 12, 2020
Revised: July 17, 2021
Accepted: July 21, 2021
Published: August 12, 2021

https://doi.org/10.1021/acs.est.0c06867
Environ. Sci. Technol. 2021, 55, 11590−11600

space and requires special permits for use in research. Furthermore, there are ethical limitations when conducting research with endangered species, since the contribution of the research to species conservation must justify the environmental impact, *i.e.*, disruption to habitat and population.[20,21] The use of toxicokinetic (TK) models, an *in silico* approach, can be a powerful alternative to *in vivo* studies with endangered species to relate internal chemical concentrations to external exposure scenarios.[22] For early-life stages (ELSs), empirically based one-compartment models are useful to obtain estimates of whole-body internal concentrations in the egg, yolk, and free-feeding stages.[23,24] For the subadult and adult life stages, a more complex mechanistic model, *i.e.*, a physiologically based toxicokinetic (PBTK) model, can be used to obtain estimates of internal concentrations in the whole fish and specific tissues during the time course of an exposure.[25,26] PBTK models use the physiological parameters cardiac output, oxygen consumption rate, and effective respiratory volume and characterize individual tissues by volume, total lipid content, total water content, and tissue perfusion rates.[26] Both model types can be integrated with parameters specific to biotransformation of an organic contaminant when applicable.[24,27,28] Additionally, the TK model framework allows for interpolation and extrapolation in relation to life stage, intraspecies, and interspecies differences in bioconcentration, and, thus, a better understanding of these differences can be obtained.

To our knowledge, until our work, there were no TK models that had been developed for white sturgeon. Additionally, there have been few studies focusing on toxicities of organic chemicals to the developmental stages of white sturgeon,[29] none of which pertain to TK. TK models developed for white sturgeon provide a tool to better understand the bioconcentration of contaminants in this species and the associated risks that the bioconcentration of chemicals might pose to its survival. The major research goal of the present study was to reparametrize existing TK models to predict the bioconcentration of organic chemicals in the embryo-larval and adult life stages of white sturgeon. Specific goals were to (a) integrate life stage-specific biotransformation into the one-compartment embryo-larval model, (b) make predictions of internal concentrations for each respective life stage, and (c) validate model predictions using measurements of B[*a*]P metabolites from exposure to graded concentrations of waterborne B[*a*]P in the embryo-larval stage and published data sets of internal organic contaminant concentrations in subadult to adult fish.

2. MATERIALS AND METHODS

2.1. Study Design. This current study was designed to provide species-specific model parameters to be integrated into two separate TK models: a one-compartment embryo-larval model and a multicompartment PBTK subadult model. As described above, the purpose of this study was to parameterize TK models for two life stages of the novel species, white sturgeon. This study was not intended to use the models to compare between life stages of white sturgeon, as the two models were validated using different chemicals and methods.

The one-compartment embryo-larval model is a reparameterization of the bioaccumulation model described by Arnot and Gobas.[30] The one-compartment embryo-larval model focused on B[*a*]P and predicting the bioconcentration of B[*a*]P metabolites throughout developmental stages, *i.e.*, eggs, yolk-sac larvae, and free-feeding stages of white sturgeon. The white sturgeon one-compartment embryo-larval model is complementary to the previously published fathead minnow one-compartment model with a focus on evaluating if the one-compartment model structure can be parameterized across species.

The subadult PBTK model is a reparameterization of the PBTK model originally designed for rainbow trout (*Oncorhynchus mykiss*)[25] and subsequently reparameterized for a multitude of other species.[24,26,31] This model was modified to include stochasticity, allowing for Monte Carlo-like simulations to be performed.[32,33] Model performance was assessed by comparing predictions to a subset of experimental values obtained from the literature, as due to the size of subadult white sturgeon and their endangered status, an *in vivo* exposure was impractical.

2.2. One-Compartment Embryo-Larval TK Model. *2.2.1. Embryo-Larval Test Organisms.* White sturgeon embryos were obtained from the Nechako White Sturgeon Conservation Centre (Vanderhoof, BC, Canada) in 2018 under the Species at Risk Act (SARA) permit 16-PPAC-00002. Embryos were immediately used in exposure experiments.

2.2.2. Embryo-Larval Waterborne B[a]P Exposure. Due to a lack of bioconcentration data in embryo-larval life stages of white sturgeon, a chronic waterborne B[*a*]P exposure was conducted for 49 days for the purpose of evaluating uptake and biotransformation of B[*a*]P and obtaining internal B[*a*]P metabolite concentrations during the egg, yolk, and free-feeding developmental stages. B[*a*]P was chosen as the model chemical as the study was designed to be complementary to a previous study conducted with fathead minnow. Nominal exposure concentrations were 1.3, 4.0, and 12.0 μg B[*a*]P/L (Sigma-Aldrich, Oakville, ON, Canada) using 0.02% DMSO (≥99.9% dimethyl sulfoxide, Fisher Scientific Co., Ottawa, ON, Canada) as the solvent carrier, 0.02% DMSO only as the solvent control, and dechlorinated laboratory water as the water control, respectively (n = 4 replicate tanks per treatment). The lower concentration of the exposure series was chosen to represent an environmentally relevant concentration. The upper end of the exposure series, while above water solubility for B[*a*]P, was chosen to induce a measurable response in the bioconcentration of B[*a*]P metabolites to act as a validation data set for the one-compartment embryo-larval white sturgeon model. Exposure details are described in the Supporting Information (SI; Section 2).

Five whole-body larvae were euthanized using buffered tricaine methanesulfonate (MS222; Acros Chemicals) on days 7, 14, 21, 28, 35, 42, and 49 of exposure, as well as after a 7 day depuration period. One larval fish (n = 4 per treatment/endpoint/sample day) was taken for biochemical and lipid analysis, as well as for analytical metabolite profiling. At each sampling point, the wet mass was recorded. The length was also recorded starting at day 21 of exposure. Samples were immediately flash-frozen in liquid nitrogen and stored at −80 °C until further analysis.

2.2.3. Embryo-Larval Biochemical Analysis. Phases I and II activity was determined through measurements of 7-ethoxyresorufin *O*-deethylase (EROD) and glutathione *S*-transferase (GST) activity, respectively. The purpose of this analysis was to evaluate metabolic responses to increasing concentrations of B[*a*]P in embryo-larval white sturgeon. Whole-body embryo-larval tissue (n = 3; one larva per treatment/sample day) was homogenized at 1 mg tissue: 20 μL of homogenization buffer to generate the postmitochondrial supernatant fraction using a

https://doi.org/10.1021/acs.est.0c06867
Environ. Sci. Technol. 2021, 55, 11590−11600

modification of the protocol described by OECD 319B.[34] Fluorescent measurements of resorufin (570 nm excitation/630 nm emission) and protein (365 nm excitation/480 nm emission) were used to determine the EROD activity (nmol mg^{-1} min^{-1}) using a modification of the protocol described by Kennedy and Jones,[35] and a kinetic measurement of 1-chloro-2,4-dinitrobenzene (CDNB; 340 nm emission) was used to determine GST activity using a modification of the protocol described by Habig et al.[36] Assay details and results are summarized in the SI (Sections 3 and 4).

2.2.4. Analytical Confirmation of Aqueous B[a]P and B[a]P Metabolites. Aqueous concentrations of B[*a*]P were analyzed loosely following the USE-EPA 525.1 method.[37] Samples of aqueous B[*a*]P (15 mL) were taken on days 7, 14, 21, 28, 35, and 49 of exposure by pooling 3.75 mL of water from replicate tanks (n = 1 per treatment). Internal standards (acenaphthene-d_{10}, chrysene-d_{12}, and phenanthrene-d_{10}; Sigma-Aldrich; 0.5 μg each) were added to the samples. Chrysene (molecular weight (MW) = 228 g mol^{-1}) was used as the internal standard for B[*a*]P (MW = 252 g mol^{-1}) because of the similar physicochemical properties. The samples were then liquid−liquid extracted by vortexing-mixing with 5 mL of dichloromethane (DCM; Sigma-Aldrich) and removing the solvent layer into a glass vial. This process was repeated three times for each sample. Solvent extracts were reduced to almost complete dryness with a gentle stream of nitrogen gas and reconstituted in 150 μL of nonane (Sigma-Aldrich). Samples were analyzed using gas chromatography-mass spectrometry (GC-MS) on a 7890A gas chromatograph with an Agilent DB-5ms (60 m × 250 μm ID, film thickness 0.1 μm) fused silica capillary column equipped with a 5975C quadrupole mass detector (Agilent Technologies). A six-point external calibration standard curve (0.1, 0.3, 0.6, 1.3, 2.5, and 5.0 μg mL^{-1}; r^2 = 0.994) was used to interpolate B[*a*]P concentrations.

The major B[*a*]P metabolites, OH-B[*a*]P and gluc-B[*a*]P, were quantified in the whole-body tissue of embryo-larval white sturgeon to generate a validation data set for the one-compartment embryo-larval model. Both metabolites were quantified with ultra-high-performance liquid chromatography high-resolution mass spectrometry (UHPLC-HRMS) in whole-body embryos using the method described by Grimard et al.[24] Briefly, whole-body embryo samples (n = 3; one larva per treatment/sample day) were homogenized in HPLC-grade acetonitrile (ACN, Fisher Scientific Co., Ottawa, ON, Canada) at a ratio of 1:10 (w/v) for 20 s. Samples were centrifuged at 1700*g* for 15 min, and the supernatant subsequently sampled for quantification of metabolites. Metabolites were analyzed using a Vanquish UHPLC and Q-Exactive HF Quadrupole-Orbitrap mass spectrometer (Thermo-Fisher, Waltham, MA), followed by ionization in negative mode heated electrospray ionization and a full MS/parallel reaction monitoring (PRM) method. OH-B[*a*]P concentrations were quantified with an analytical standard and external calibration, and a semi-quantitative method was used to quantify gluc-B[*a*]P in which a response factor was used to convert peak areas of OH-B[*a*]P to peak areas of gluc-B[*a*]P. Final B[*a*]P metabolite concentrations (ng mg whole-body $larvae^{-1}$ and μM) were calculated from the volume of solvent used for extraction.

2.2.5. One-Compartment Embryo-Larval Model Parameterization. Parameterization of the embryo-larval model (Table 1 and Supporting Table S2) included experimental values for wet mass, whole-body total lipid content, and whole-body biotransformation rate (k_{MET}).

Table 1. Physiological Parameters Used in the One-Compartment Model for Embryo-Larval White Sturgeon (*A. transmontanus*)

life stage (dpf[a])	wet mass (mg ± SD)	lipid (% of wet mass)	k_{MET} (1/d)[b]
7	49.11 ± 10.61	2.85 ± 0.42	0.0016
12	32.30 ± 6.78	3.62 ± 0.91	0.0013
21	40.09 ± 6.45	2.99 ± 0.71	0.0015
35	49.38 ± 8.51	2.54 ± 1.48	0.0019
42	59.5 ± 15.83	1.38 ± 0.16	0.0033
49	82.60 ± 27.88	0.47 ± 0.32	0.0097
56	124.15 ± 36.63	0.25 ± 0.16	0.0183

[a]Days post fertilization. [b]Whole-body biotransformation; internally calibrated.

The wet mass was measured directly at the time of euthanasia. Total whole-body lipid content was quantified using a modification of the microcolorimetric sulfophospho-vanillin (SPV) protocol described by Lu et al.[38] Lipids were extracted from whole-body embryo-larval fish (n = 4; one larva per treatment/sampling point). Lipid extracts were quantified by the addition of sulfuric acid and the SPV reagent. The lipid content (mg) was determined through measurements of absorbance using cod liver oil as the standard, and the lipid fraction was subsequently calculated. Additional assay details are defined in the SI (Section 6).

Whole-body biotransformation was calibrated using the measured whole-body B[*a*]P metabolite concentrations. While this was not the preferred method, it was not possible to accurately scale embryo-larval k_{MET} from the measurements of subadult biotransformation (0.219 ± 0.070 mL h^{-1} mg $protein^{-1}$, SI Section 5; Figure S6), as done in previous studies.[24] The reason why allometric scaling from subadult biotransformation was not possible in this case is because the embryo-larval white sturgeon showed unexpectedly very low biotransformation activity. Model predictions using the allometrically scaled k_{MET} value resulted in vast overpredictions and it was concluded that for white sturgeon, biotransformation was not scalable between life stages as shown previously for fathead minnow.[24] Due to a lack of methods to directly measure k_{MET} in embryo-larval fish, it was decided that the most appropriate approach would be to calibrate k_{MET} for the embryo-larval stage of white sturgeon. It should be noted that both the allometric scaling and the calibration method should be considered when parameterizing the one-compartment embryo-larval model for other species.

Calibration of k_{MET} was performed using the measured whole-body B[*a*]P metabolite concentrations. Using 42 data points, a randomly generated train-test split was generated in Microsoft Excel 16.30 (Microsoft Co., Redmond, WA) using the randomize function to assign each data point a random number and sorting the data points by their randomly assigned number. The first half of the data in the sorted list were used to train (calibrate) k_{MET} and the second half of the data in the sorted list were used to test the calibrated k_{MET} value. Calibration of k_{MET} was conducted by adjusting k_{MET} in the embryo-larval model until the largest percentage of predictions within 1 order of magnitude of the training set of measured values was achieved (Supporting Figure S9). Test values for

https://doi.org/10.1021/acs.est.0c06867
Environ. Sci. Technol. 2021, 55, 11590−11600

k_{MET} were obtained by scaling *in vitro* clearance to whole-body biotransformation using a scaling equation (Supporting Table S1) and estimates of cardiac output. Since it is difficult to measure cardiac output directly in embryo-larval white sturgeon, estimates of cardiac output from embryo-larval fathead minnow (*Pimephales promelas*) were used.[24] Multiple test values for *in vitro* clearance were used to identify a value that results in a k_{MET} value that would best represent the whole-body biotransformation rate of embryo-larval white sturgeon. Test values for *in vitro* clearance included the lowest observable detection (LOD) value and half the LOD from the OECD 319B intrinsic clearance assay[34] and the value for subadult white sturgeon *in vitro* clearance (0.219 mL h^{-1} mg^{-1}; SI Section 5) scaled down between 50 and 300 times. The resulting calculated k_{MET} values obtained from implementing the test *in vitro* clearance values into a scaling equation were tested in the model until the greatest number of predictions were within 10-fold of measured values. Equations used for determination of k_{MET} were obtained from Nichols et al.[27] and are summarized in the SI (Supporting Table S1).

2.2.6. One-Compartment Embryo-Larval Model Implementation and Evaluation. All model parameters and equations are summarized in the SI (Section 7). The one-compartment embryo-larval model applied measured wet mass, lipid contents, and the calibrated k_{MET} values. The model was used to predict the abundance of B[*a*]P metabolites (eq S21). Embryo-larval model predictions were compared to measured abundances of B[*a*]P metabolites (Figure S4) from the embryo-larval B[*a*]P exposure. Since there is limited information regarding proportions of B[*a*]P metabolites in embryo-larval model, all model predictions were assumed to represent OH-B[*a*]P and its associated glucuronide entirely. This conclusion is supported by a study conducted with zebrafish where glucuronidation was shown to be the main pathway in the embryo-larval life stage.[39] In cases where other metabolites are measured or more information regarding metabolite proportions is available, then consideration of metabolite proportions should be given when parameterizing the one-compartment embryo-larval model for other species.

2.3. Subadult PBTK Model. *2.3.1. Subadult Test Organisms.* Subadult white sturgeons were raised in the Aquatic Toxicology Research Facility at the University of Saskatchewan from embryos originally obtained from the Nechako White Sturgeon Conservation Centre in 2013 under the SARA permit XRSF-20-2013.

2.3.2. Subadult PBTK Model Parameterization. The subadult PBTK model (Table 2 and Supporting Table S4) required parameterization of tissue volume, lipid, and moisture content for each model compartment, *i.e.*, fat, liver, poorly perfused tissues, and richly perfused tissues, in addition to the parametrization of the physiological components: cardiac output, oxygen consumption, and effective respiratory volume.

2.3.2.1. Subadult Tissue Volumes, Lipid Content, and Moisture Content. Volumes of eight tissues from the subadult white sturgeon were determined in a total of 11 fish. The sampled tissues consisted of liver, kidney, spleen, muscle, brain, gills, viscera, and carcass, *i.e.*, the tissue remaining after all other tissues had been sampled. The tissues were weighed, and volumes were determined from the wet mass by assuming all tissues had a specific density of 1.0 g mL^{-1}. Tissues were stored at −20 °C until further analysis of the lipid and the moisture content.

Table 2. Physiological Parameters Used in the PBTK Model for Subadult White Sturgeon (*A. transmontanus*)[a]

parameter	description	value (mean ± SD)
W	body wet mass (kg)	model input
Q_c	cardiac output (L kg^{-1} h^{-1})	calculated
VO_2	oxygen consumption rate (mg kg^{-1} h^{-1})	calculated
Q_w	effective respiratory volume (L kg^{-1} h^{-1})	calculated
	Compartment Volumes (L)	
V_l	volume of the liver compartment	0.029 ± 0.004
V_m	volume of poorly perfused tissues	0.894 ± 0.013
V_r	volume of richly perfused tissues	0.058 ± 0.010
V_f	volume of the fat compartment	calculated
	Arterial Blood Flow to Compartments (Fraction of Cardiac Output)	
Q_l	arterial blood flow to liver compartment	0.071 ± 0.025
Q_m	arterial blood flow to poorly perfused tissues	0.717 ± 0.175
Q_r	arterial blood flow to richly perfused tissues	0.202 ± 0.156
Q_f	arterial blood flow to fat compartment	0.010 (assumed)
	Lipid Content of Tissue Compartments (Fraction of Body Wet Mass)	
α_l	lipid content of the liver compartment	0.306 ± 0.078
α_m	lipid content of poorly perfused tissues	0.026 ± 0.009
α_r	lipid content of richly perfused tissues	0.014 ± 0.007
α_f	lipid content of the fat compartment	0.522 ± 0.168
	Water Content of Tissue Compartments (Fraction of Body Wet Mass)	
γ_l	water content of the liver compartment	0.510 ± 0.057
γ_m	water content of poorly perfused tissues	0.757 ± 0.022
γ_r	water content of richly perfused tissues	0.848 ± 0.029
γ_f	water content of the fat compartment	0.342 ± 0.217

[a]Values were determined from n = 11, 3 year old fish with a body length of 40.6 ± 2.74 cm and a wet mass of 510 ± 105 g.

Total whole-body lipid content in both life stages was quantified. Lipids were extracted from each sampled tissue in the adult fish (n = 11 individuals) using a modification of the microcolorimetric sulfophosphovanillin (SPV) protocol as described above for the embryo-larval study. Additional assay details are defined in the SI (Section 6).

A subsample of the tissue samples was dried in an oven at 105 °C for 24 h to determine the total moisture content (%) for each sampled tissue of the subadult fish (n = 11 individuals).

2.3.2.2. Subadult Tissue Perfusion and Cardiac Output. Cardiac output and tissue perfusion rates were measured in four subadult white sturgeon. First, the fish were anesthetized with a 10 mg L^{-1} solution of Aquacalm (Syndel; Nanaimo, BC, Canada). A continual flow of aerated water at 13 °C containing the same anesthetic solution was dispensed through the mouth of the fish to maintain anesthesia and oxygenation throughout the duration of the procedures.

Cardiac output (n = 4 individuals) was measured using the protocol described by Pettem et al.,[40] using a Vevo3100 ultrasound system (FujiFilm VisualSonics, Toronto, ON, Canada) with an MX250 transducer capable of pulse-wave Doppler and B-mode imaging. The fish were restrained ventral side up in a foam holder for imaging of the cardiac area. Measurements of systolic and diastolic volume were used to determine the ventricular stroke volume (V_S), and measurements of ventricular contractile rates (f_H) were manually counted (bpm). Cardiac output was calculated as $f_H \times V_S$.

Tissue perfusion rates (n = 4 per tissue) were measured using fluorescently labeled microspheres. A heparinized catheter was used to cannulate the dorsal aorta in the roof of

https://doi.org/10.1021/acs.est.0c06867
Environ. Sci. Technol. 2021, 55, 11590−11600

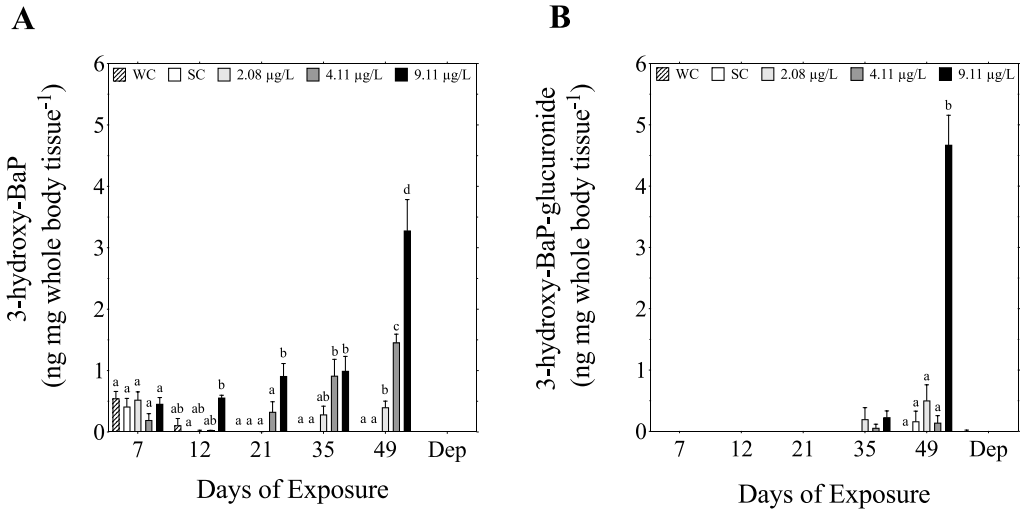

Figure 1. Abundance of 3-OH-B[*a*]P (A; ng mg whole-body tissue^{-1}) and 3-OH-B[*a*]P-glucuronide (B; ng mg whole-body tissue^{-1}) in whole-body embryo-larval white sturgeon after 7, 12, 21, 35, and 49 days of exposure to increasing concentrations of B[*a*]P and the water control (WC) and the solvent control (SC). Data are expressed as mean ± standard error of the mean (SEM). Different letters denote a significant difference in B[*a*]P metabolites between treatment groups within each respective time point. No letters indicate no significant differences between treatment groups within the respective time point (nonparametric analysis: Kruskal–Wallis with Dunn's multiple comparison test, $\alpha = 0.05$; parametric analysis: one-way ANOVA with Tukey's HSD, $\alpha = 0.05$). No abundance of gluc-B[*a*]P was measured on 7, 12, or 21 days of exposure.

the mouth. The catheter was injected at a volume of 1 mL per kg fish with a saline solution containing a nominal count of 500 000 pink NuFlow Hydro-Coat microspheres (15.5 ± 1.1 μm diameter, NuFlow Microspheres, Smithville, MO), and 30 min was allotted for microsphere tissue distribution. After 30 min, the fish were euthanized with an overdose of metomidate (Syndel, Ferndal, WA), and the liver, spleen, muscle, brain, gills, viscera, and carcass were dissected. Microspheres were extracted using the NuFlow Fluorescent Microsphere Extraction protocol with yellow NuFlow Hydro-Coat microspheres as the recovery standard. Using an Accuri C6 flow cytometer (BD Bioscience, San Jose, CA), microspheres were counted. The number of recovery microspheres (yellow) was used to correct for the number of target microspheres (pink), which were further scaled to total tissue volume, and tissue perfusion was calculated as a fraction of cardiac output.

2.3.2.3. Subadult Oxygen Consumption Rate and Effective Respiratory Volume. Data for oxygen consumption rate ($n = 4$ individuals) were generated from active fish values listed in the metabolism table of the FishBase database (www.fishbase.org)[41] for white sturgeon. Effective respiratory volume was calculated using the equation described in a previously published PBTK model for rainbow trout.[26]

2.3.3. Subadult PBTK Model Implementation and Evaluation. All model parameters and equations are summarized in the SI (Section 8). The subadult PBTK model used measured values for tissue volume, lipid content, moisture content, and tissue perfusion parameters. The parameters were implemented with stochasticity by providing the model with the average parameter value along with the standard deviation to represent the range in parameter values. Monte Carlo-like simulations (200 simulations per data point) were run in which a random combination of parameter values from each parameter distribution was chosen, assuming that the parameters were independent.

An experimental data set of bioconcentration data in subadult white sturgeon was used to validate the subadult PBTK model predictions as an *in vivo* study would have been impractical. To obtain the experimental validation data set, a search was performed using the University of Saskatchewan Library database. Keywords (their variations) and their combinations included bioaccumulation, bioconcentration, contaminants, organics, toxicokinetics, uptake, and white sturgeon. Four published data sets were retrieved that included internal concentrations and muscle concentrations for sturgeon exposed to the organic contaminants avermectin-B1,[42] molinate,[43] sulfamethazine (SM_2),[44] and *p*-nitrophenol (PNP).[45] As experimental TK data are limited for white sturgeon, two of the experimental data sets (avermectin-B1 and SM_2) pertained to Chinese sturgeon, and we assumed that the two species would be physiologically similar. The subadult PBTK model predictions were not intended to be compared and evaluated against the results of the one-compartment embryo-larval white sturgeon model study.

2.4. Statistical Analysis. A one-way ANOVA or Kruskal–Wallis test was used to assess the differences in B[*a*]P metabolite concentrations among treatment groups within time points from the embryo-larval B[*a*]P exposure. Data were evaluated for normality (D'Agostino–Pearson test) and heterogeneity of variance (Brown–Forsythe test), and log-transformed to meet normality assumptions, when necessary. An unpaired t-test was used to determine if a difference existed between the modeled and the measured or literature values for subadult cardiac output and oxygen consumption, respectively. Significant differences were defined by $p \leq 0.05$. All statistical tests were performed using GraphPad Prism 8 (GraphPad Software, Inc., San Diego, CA). RMSE (root mean squared error) calculations were performed to evaluate model performance using Microsoft Excel 16.30 (Microsoft Co.).

3. RESULTS AND DISCUSSION

3.1. Embryo-Larval Exposure and One-Compartment Model. *3.1.1. Embryo-Larval Aqueous B[a]P Exposure Concentrations.* Mean measured aqueous B[*a*]P concentrations (± SD) for the embryo-larval exposure were 2.08 (±1.59), 4.11 (±2.61), and 9.11 (±3.54) μg B[*a*]P/L. There

https://doi.org/10.1021/acs.est.0c06867
Environ. Sci. Technol. 2021, 55, 11590–11600

were no observed effects on growth or mortality at these measured concentrations.

Higher concentrations compared to nominal concentrations in the two lower test concentrations is likely a result of variations in stock solution preparations and scale calibrations. Sorption to the exposure aquaria and particulates, incomplete solubility, and degradation likely resulted in the reduced B[*a*]P concentration observed in the highest exposure concentration. While variations in B[*a*]P concentrations are not ideal, the exposure concentrations were great enough to produce a measurable response in whole-body metabolite concentrations. Therefore, while consideration must be given to the variation in aqueous test concentrations, the exposure results can be used for validation of the model predictions.

3.1.2. Embryo-Larval B[a]P Metabolite Concentrations. Results of B[*a*]P metabolite analysis showed an increasing trend in abundance of both OH-B[*a*]P and Gluc-B[*a*]P with time and exposure concentration. A significant increase in OH-B[*a*]P was observed at 12 (χ^2 = 9.593, df = 5, p = 0.0207), 21 (one-way ANOVA, F = 11.68, p = 0.0009), 35 (one-way ANOVA, F = 8.211, p = 0.0033), and 49 (one-way ANOVA, F = 88.75, p < 0.0001) days of exposure (Figure 1A). Likewise, a significant increase was observed in gluc-B[*a*]P at 49 days of exposure (one-way ANOVA, F = 60.02, p < 0.0001; Figure 1B). The measured abundances of B[*a*]P metabolites were significantly less than what has been reported in fathead minnow larvae at the same life stage.[24] Additionally, in the present study, no detectable abundance of gluc-B[*a*]P was measured on days 7, 12, or 21 of exposure, despite showing some phase II (GST) activity during the early developmental stages (Supporting Figure S3). Because glucuronide is the primary metabolite resulting from biotransformation of OH-B[*a*]P by the enzyme glucuronosyltransferase (UGT),[46] this observation may be indicative of the absence of or limitation in UGT activity during the first developmental phases of white sturgeon.

To our knowledge, there is no information regarding uptake and biotransformation of B[*a*]P in white sturgeon. In the present study, the embryo-larval white sturgeon showed slightly greater whole-body lipid content during the egg and yolk-sac stages comparative to other fish species;[23,24] however, during the free-feeding stage, the whole-body lipid content decreased significantly (Table 1). Compared to other species at the free-feeding stage, such as fathead minnow[24] and common sole (*Solea solea*),[23] which have a whole-body lipid content averaging 2.84 and 2.45%, respectively, and adult white sturgeon, which have a whole-body lipid content of 10% (Table S4), free-feeding white sturgeon in this study exhibited a substantially lesser whole-body lipid content (0.25−1.38%). The decrease in the lipid content is likely a result of a rapid increase in growth observed in the free-feeding stage. Because the lipid content is one of the main drivers of uptake for lipophilic compounds,[47−49] such as B[*a*]P, the low lipid content measured in the embryo-larval white sturgeon likely contributed to a lesser uptake of B[*a*]P from the water column compared to other species. Accordingly, a lesser uptake in B[*a*]P results in a less available parent compound for biotransformation. In addition, white sturgeon have been shown to have slower rates of biotransformation compared to other species.[50] Therefore, limited uptake in combination with slow rates of biotransformation likely contributed to the reduced B[*a*]P metabolite abundances. As a result, embryo-larval, white sturgeon are more likely subject to the teratogenic[51,52] effects associated with AhR binding when exposed to B[*a*]P, rather than the genotoxic effects associated with the formation of toxic metabolites.[53,54]

3.1.3. Embryo-Larval Model Parameterization and Performance. The white sturgeon one-compartment embryo-larval model was parameterized using direct measurements of wet mass and lipid content and calibrated k_{MET} rates. No difference in phase I (EROD) or II (GST) activity was observed in the embryo-larval white sturgeon with exposure to increasing concentrations of B[*a*]P (SI Figures S2 and S3), which indicates that no saturation of biotransformation enzymes occurred. Therefore, it was assumed that our exposure concentrations were within the first-order portion of the Michaelis−Menten model and biotransformation increased proportionally with the exposure concentration. This is advantageous as only one k_{MET} value would need to be applied versus several to account for saturation. The concept of first-order biotransformation kinetics was further explored when the embryo-larval model was parameterized for fathead minnow.[24]

Values for k_{MET} were scaled from an *in vitro* clearance value of 0.00078 mL h^{-1} mg $protein^{-1}$ (Table 1). The major limitation to generating accurate predictions of B[*a*]P metabolites with the one-compartment embryo-larval model is accurately parameterizing k_{MET}. In the present study, when k_{MET} was allometrically scaled from *in vitro* intrinsic clearance measured directly from subadult white sturgeon livers (0.219 mL h^{-1} mg^{-1}, SI Section 5), model predictions were greatly overestimated (>100-fold; SI Figure S6). Similarly, a large overprediction was observed when k_{MET} was scaled using the LOD (0.05 mL h^{-1} mg $protein^{-1}$; SI Figure S7) and half the LOD value for the *in vitro* clearance assay (0.025 mL h^{-1} mg $protein^{-1}$; SI Figure S8).[34] We could not attribute the overpredictions to differences in the fractional liver volume or blood flow parameters, used in the IVIVE equations, between the embryo-larval and subadult life stages. Therefore, it was determined that the most appropriate method to estimate biotransformation in white sturgeon would be to internally calibrate k_{MET} using half our measured metabolite abundance data points. While this method might result in some inaccuracies in the model predictions, due to the lack of available methods, it was not possible to directly measure this parameter.

Whole-body concentrations of B[*a*]P metabolites were predicted using the one-compartment embryo-larval model. A significant correlation was observed between the measured metabolite abundances and the predicted values from the one-compartment embryo-larval model. The model displayed good predictive power, with 62% of predictions deviating less than five-fold of the measured values and 81% of the predictions deviating less than 10-fold of the measured values (Figure 2). An RMSE of 0.47 log units was calculated, which is slightly lower than when this model was used to make predictions of B[*a*]P metabolites in embryo-larval fathead minnow (0.64 log units).[24]

The training data showed a greater number of predictions (86%) within 1 order of magnitude (Supporting Figure S9) compared to the test data set, with a RMSE (0.53 log units) similar to the test data set. In the test data set, the discrepancies were a result of two data points that were greatly overpredicted and two data points that were greatly underpredicted. These data points are likely a result of individual differences in uptake and biotransformation and

https://doi.org/10.1021/acs.est.0c06867
Environ. Sci. Technol. 2021, 55, 11590−11600

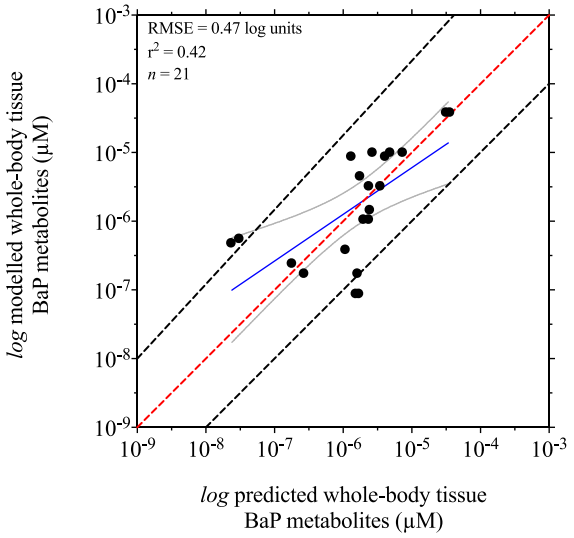

Figure 2. Relationship between predicted and measured concentrations of whole-body tissue B[*a*]P metabolites (μM) using the test data set of 21 data points for validation. The red dashed line represents the equality line, the black dashed lines represent the ±10-fold deviation from equality, and the solid blue line represents a linear regression with associated 95% confident intervals (gray). RMSE, root mean squared error.

represent the extremes on both sides of the spectrum. Additional limitations to consider are the variable aqueous B[*a*]P concentrations and proportions of B[*a*]P metabolites. The one-compartment embryo-larval model used in this study assumed that the predicted metabolite abundance is represented entirely by the OH-B[*a*]P and associated glucuronide. While glucuronidation has been identified as the main biotransformation pathway in embryo-larval zebrafish,[39] it is known that B[*a*]P is biotransformed into many different metabolites[45] and it is likely that metabolite proportions differ between species. Therefore, the observed overpredictions might be a result of not accounting for the proportion of OH-B[*a*]P and associated glucuronide from the total metabolite concentration. To mitigate this limitation, a future consideration could be measuring parent B[*a*]P directly with advanced analytical methods to determine critical body residues[55] in the whole-body embryo-larval samples, rather than B[*a*]P metabolites, and comparing directly to whole-body parent B[*a*]P predictions from the model. B[*a*]P metabolites were chosen in the current study as, per the resources available, they were easy to measure and provided a good biomarker of exposure.

When the test data set was plotted against exposure time (Supporting Figure S10), it was observed that discrepancies occurred particularly during the first two phases of development, *i.e.*, the egg and yolk-sac stage. This result is comparable to what has been observed previously when this model was used to predict B[*a*]P metabolites in embryo-larval fathead minnow.[24] In fathead minnow, it was concluded that biotransformation was underestimated during the egg and yolk-sac stages of development as an underprediction of B[*a*]P metabolites was observed. Results of studies with zebrafish larvae have shown that extensive biotransformation can occur as soon as gastrulation;[39,56] therefore, it is likely that biotransformation in the embryo-larval stage is greater at the onset of development than what was calculated. The observations in embryo-larval white sturgeon support this conclusion during the egg stage; however, a trend of overpredictions was observed during the yolk-sac stage. Discrepancies in embryo-larval biotransformation highlight the need for methods to directly measure this parameter in the embryo-larval life stage. Additionally, because B[*a*]P toxicity can be elicited either by AhR binding and/or through the generation of toxic metabolites, the extent of biotransformation in the embryo-larval life stage must be better understood to make accurate conclusions of the cause of toxicity.

3.2. Subadult PBTK Model. *3.2.1. Subadult Model Parameterization and Performance.* A subadult PBTK model for white sturgeon was developed to predict the bioconcentration of organic contaminants. Parameterization of tissue volume, lipid content, and water content was determined experimentally, and the measured values were directly implemented in the model (Table 2). The modeled value for cardiac output did not significantly differ from the measured values (*t*-test, $t_6 = 0.4067$, $p = 0.6983$). Likewise, the modeled value for oxygen consumption did not significantly differ from the literature values (*t*-test, $t_6 = 0.9207$, $p = 0.3927$), which indicates that the scientific literature data was sufficient for model parameterization.

An experimental data set, comprising 39 data points, was compiled for evaluation of the subadult white sturgeon model. This data set consisted of measured internal or muscle concentrations from white or Chinese sturgeon that were aqueously exposed to various organic contaminants ranging in log K_{ow}s from 0.53 to 4.40. Specific exposure conditions, *i.e.*, chemical concentrations, temperature, dissolved oxygen, and fish mass, were also included (Supporting Table S3). The subadult PBTK model showed relatively good performance with 59% of predicted values deviating less than five-fold from the measured values, and 90% of predicted values deviating less than 10-fold from the measured values (Figure 3). Additionally, the model had an RMSE of 0.68 log units, and the r^2 was 0.81. The model performed equally well compared to models for other species of fish.[24,26,31]

PNP and molinate showed the most accurate predictions with all data points deviating less than five-fold from equality. The experimental data sets for both chemicals were specific to white sturgeon, and therefore, a satisfactory level of confidence that our model is accurately parameterized for this species was obtained. It should be recognized, however, that only one data point was available for molinate after a depuration period, and definitive conclusions on the performance of the model in regard to the uptake of this chemical cannot be made. SM_2 had relatively accurate predictions, except for one data point that was largely overpredicted. Overprediction occurred for a data point measured at the beginning of exposure (6 h) and indicated that the model-simulated rate of uptake was faster than the measured rate. Avermectin-B1 showed consistent overpredictions of approximately 10-fold for all data points. Data sets for both SM_2 and avermectin-B-1 were obtained from the Chinese sturgeon. Therefore, interspecies differences in physiology, such as differences in the lipid content of the tissues (*i.e.*, Chinese sturgeon liver lipid content = 12.2–12.7%;[57,58] white sturgeon lipid content = 30.6% (SI Table S4)), might have contributed to the observed discrepancies.

3.2.1.1. p-Nitrophenol. PNP originates as a residue of organophosphates and elicits toxicity primarily through mitochondrial oxidative phosphorylation.[45,59] While PNP can be actively biotransformed, it was observed that aquatic

https://doi.org/10.1021/acs.est.0c06867
Environ. Sci. Technol. 2021, 55, 11590−11600

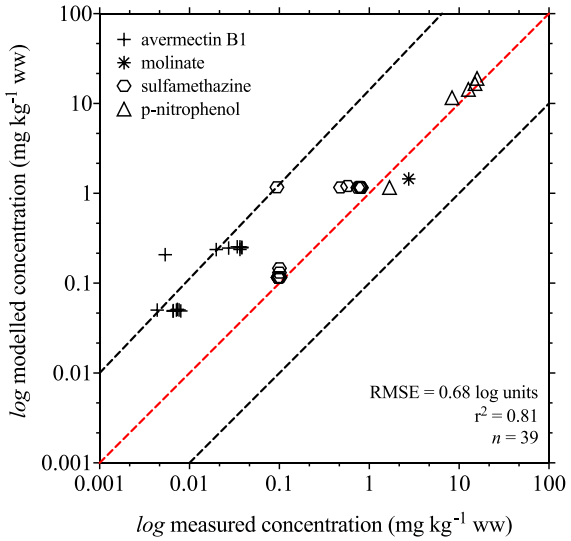

Figure 3. Relationship between measured and modeled internal concentrations of avermectin-B1, molinate, sulfamethazine, and *p*-nitrophenol in subadult white sturgeon. The red dashed line represents the equality line, and the black dashed lines represent the ±10-fold deviation from equality. RMSE, root mean squared error.

organisms, including white sturgeon, can depurate the majority of parent PNP unchanged. It was concluded, however, that extensive biotransformation is possible when required.[45] In the present model, biotransformation of PNP was not included. While the integration of biotransformation could improve model outputs in some PNP exposure scenarios, our data show that it is not necessary in all cases.

3.2.1.2. Molinate. Molinate is a commonly used herbicide that is leached into groundwater and subsequently rivers and lakes.[43,60] Similar to B[*a*]P, molinate is actively biotransformed;[43,61,62] however, biotransformation of molinate was not included in the model. The experimental data set provided only a single data point after 24 h of depuration. Our data show that for this exposure scenario, the PBTK model could accurately predict the depuration of the parent compound, and a biotransformation parameter was not needed. It is possible, as shown with other chemicals,[49] that white sturgeon have limited biotransformation capacity for molinate. Integration of biotransformation might be necessary, however, for other species.

3.2.1.3. Avermectin-B1. Avermectin-B1 is a widely used pesticide that can be leached into nearby bodies of water.[42,63] In fish, avermectin-B1 shows minimal bioconcentration[63,64] and is not readily biotransformed.[40] Therefore, it is unlikely that the absence of biotransformation in the model contributes to the overpredictions. Instead, it is suggested that the large molecular size of avermectin-B1, which is not represented in the model, inhibits membrane permeability and subsequently bioconcentration.[64−66] Additionally, it has been shown that interspecies differences in kinetics exist for avermectin-B1.[42] Therefore, it is possible that differences between Chinese and white sturgeon also contributed to the inaccuracies in model predictions.

3.2.1.4. Sulfamethazine. SM_2 is a multipurpose agricultural product used as a growth promoter and prophylactic treatment in production animals that can be excreted and contaminate the surrounding water bodies.[44,67] In fish, the compound has been shown to have acute toxicity, reproductive effects, and alter biochemical, hematological, and antioxidant responses.[68,69] SM_2 is an ionizable chemical that is primarily biotransformed into N^4-acetyl-SM_2.[44] A molecule in its ionized state cannot readily permeate across membranes. The chemical's acid dissociation constant (pKa) described by the pH in which 50% of molecules are ionized influences the extent of chemical ionization.[48] Therefore, bioconcentration of ionizable compounds is shown to be difficult to predict as the ambient pH affects the extent of uptake.[31,44,70] The absence of biotransformation in the model might be a contributing factor to the observed overpredictions.

3.3. Conclusions and Further Directions. The present study parameterized and validated a one-compartment embryo-larval model and a subadult PBTK model for the uptake and biotransformation of organic chemicals in white sturgeon. Both models were shown to be accurate, with 81−90% of predictions within 10-fold of measured values. However, the parameterization of biotransformation remains a limitation to the current models. For the embryo-larval model, further research should pertain to developing techniques to measure embryo-larval specific biotransformation rates.[71,72] Additionally, further studies that focus on derivation of k_{MET} in other fish life stages are warranted. In the subadult stages, the data sets regarding chemical-specific biotransformation in white sturgeon should continue to be expanded. While the models described in this study focused explicitly on aqueous uptake of organic compounds, an additional limitation that should be considered for future TK models is parameterizing the current TK models to consider the influence of dietary intake as has been conducted previously for zebrafish.[73,74]

As white sturgeon are presently an endangered species in northwestern Canadian and U.S. rivers, TK models are particularly advantageous as they can be used to simulate exposure scenarios when *in vivo* assessment is unethical or impractical. Using TK models in this context can support risk assessment in this species by allowing for a better understanding of chemical bioconcentration and the concentrations that reach the target tissues. Furthermore, the power of TK models for white sturgeon could be further improved if combined with toxicodynamic (TD) models to create a TK−TD model framework, allowing for predictions of both chemical bioconcentration and associated effects. The models presented in this research must continue to be tested against more chemicals and exposure scenarios to broaden the understanding of the kinetics of contaminants in white sturgeon and the influence that the bioconcentration of such chemicals might have on their health and survival.

■ ASSOCIATED CONTENT

Supporting Information

The Supporting Information is available free of charge at https://pubs.acs.org/doi/10.1021/acs.est.0c06867.

Additional methodology regarding the embryo-larval B[*a*]P exposure; biochemical analyses; analytical metabolite quantification; lipid quantification; intrinsic clearance measurements; one-compartment and PBTK models; tables showing the model inputs and parameters; and model equations (PDF)

https://doi.org/10.1021/acs.est.0c06867
Environ. Sci. Technol. 2021, 55, 11590−11600

AUTHOR INFORMATION

Corresponding Author

Markus Hecker − *Toxicology Centre, University of Saskatchewan, Saskatoon, Saskatchewan S7N 5B3, Canada; School of Environment and Sustainability, University of Saskatchewan, Saskatoon, Saskatchewan S7N 5C8, Canada;* Email: markus.hecker@usask.ca

Authors

Chelsea Grimard − *Toxicology Centre, University of Saskatchewan, Saskatoon, Saskatchewan S7N 5B3, Canada;* orcid.org/0000-0002-8189-0599

Annika Mangold-Döring − *Toxicology Centre, University of Saskatchewan, Saskatoon, Saskatchewan S7N 5B3, Canada; Institute for Environmental Research (Biology V), RWTH Aachen University, Aachen 52074, Germany;* orcid.org/0000-0002-6701-308X

Hattan Alharbi − *Department of Plant Protection, College of Food and Agriculture Sciences, King Saud University, Riyadh 11451, Saudi Arabia;* orcid.org/0000-0003-3297-729X

Lynn Weber − *Toxicology Centre, University of Saskatchewan, Saskatoon, Saskatchewan S7N 5B3, Canada; Department of Veterinary Biomedical Sciences, University of Saskatchewan, Saskatoon, Saskatchewan S7N 5B4, Canada*

Natacha Hogan − *Toxicology Centre, University of Saskatchewan, Saskatoon, Saskatchewan S7N 5B3, Canada; Department of Animal and Poultry Science, College of Agriculture and Bioresources, University of Saskatchewan, Saskatoon, Saskatchewan S7N 5A8, Canada*

Paul D. Jones − *Toxicology Centre, University of Saskatchewan, Saskatoon, Saskatchewan S7N 5B3, Canada; School of Environment and Sustainability, University of Saskatchewan, Saskatoon, Saskatchewan S7N 5C8, Canada*

John P. Giesy − *Toxicology Centre, University of Saskatchewan, Saskatoon, Saskatchewan S7N 5B3, Canada; Department of Veterinary Biomedical Sciences, University of Saskatchewan, Saskatoon, Saskatchewan S7N 5B4, Canada; Department of Environmental Sciences, Baylor University, Waco, Texas 76706, United States*

Markus Brinkmann − *Toxicology Centre, University of Saskatchewan, Saskatoon, Saskatchewan S7N 5B3, Canada; School of Environment and Sustainability, University of Saskatchewan, Saskatoon, Saskatchewan S7N 5C8, Canada; Global Institute for Water Security, University of Saskatchewan, Saskatoon, Saskatchewan S7N 3H5, Canada;* orcid.org/0000-0002-4985-263X

Complete contact information is available at: https://pubs.acs.org/10.1021/acs.est.0c06867

Notes

The authors declare no competing financial interest.

ACKNOWLEDGMENTS

All fish culture protocols and experimental procedures for both the embryo-larval and subadult experiments were approved by the Animal Research Ethics Board at the University of Saskatchewan (Protocol #20070049). Funding was provided through an NSERC Discovery Grant to Dr. M.H. Dr. M.B. was supported through the Canada First Research Excellence Funds Global Water Futures program led by the University of Saskatchewan, and a Banting Postdoctoral Fellowship through NSERC. Drs. J.P.G. and M.H. were supported through the Canada Research Chairs program. H.A. was supported through the project number (RSP-2020/128), King Saud University, Riyadh, Saudi Arabia. The graphical abstract and Figure S1 were created with BioRender.com.

REFERENCES

(1) McAdam, S. O.; Walters, C. J.; Nistor, C. Linkages between white sturgeon recruitment and altered bed substrates in the Nechako River, Canada. *Trans. Am. Fish. Soc.* **2005**, *134*, 1448−1456.

(2) McAdam, S. O. Effects of substrate condition on habitat use and survival by white sturgeon (*Acipenser transmontanus*) larvae and potential implications for recruitment. *Can. J. Fish. Aquat. Sci.* **2011**, *68*, 812−822.

(3) Paragamian, V. L.; McDonald, R.; Nelson, G. J.; Barton, G. Kootenai River velocities, depth, and white sturgeon spawning site selection−a mystery unraveled? *J. Appl. Ichthyol.* **2009**, *25*, 640−646.

(4) Feist, G. W.; Webb, M. A.; Gundersen, D. T.; Foster, E. P.; Schreck, C. B.; Maule, A. G.; Fitzpatrick, M. S. Evidence of detrimental effects of environmental contaminants on growth and reproductive physiology of white sturgeon in impounded areas of the Columbia River. *Environmen. Health Perspect.* **2005**, *113*, 1675−1682.

(5) Greenfield, B. K.; Davis, J. A.; Fairey, R.; Roberts, C.; Crane, D.; Ichikawa, G. Seasonal, interannual, and long-term variation in sport fish contamination, San Francisco Bay. *Sci. Total Environ.* **2005**, *336*, 25−43.

(6) Gundersen, D. T.; Webb, M. A. H.; Fink, A. K.; Kushner, L. R.; Feist, G. W.; Fitzpatrick, M. S.; Foster, E. P.; Schreck, C. B. Using blood plasma for monitoring organochlorine contaminants in juvenile white sturgeon, *Acipenser transmontanus*, from the lower Columbia River. *Bull. Environ. Contam. Toxicol.* **2008**, *81*, 225−229.

(7) Gundersen, D. T.; Zeug, S. C.; Bringolf, R. B.; Merz, J.; Jackson, Z.; Webb, M. A. Tissue contaminant burdens in San Francisco Estuary White Sturgeon (*Acipenser transmontanus*): implications for population recovery. *Arch. Environ. Contam. Toxicol.* **2017**, *73*, 334−347.

(8) MacDonald, D. Contaminants in white sturgeon (*Acipenser transmontanus*) from the upper Fraser River, British Columbia, Canada. *Environ. Toxicol. Chem.* **2009**, *16*, 479−490.

(9) COSEWIC. *COSEWIC Assessment and Status Report on the White Sturgeon Acipenser transmontanus in Canada*; Committee on the Status of Endangered Wildlife: Ottawa, Canada, 2012; xxvii, p 75.

(10) U.S. Fish and Wildlife Service. *Recovery Plan for the White Sturgeon (Acipenser transmontanus): Kootenai River Population*; U.S. Fish and Wildlife Service: Portland, Oregon, 1999; p 96, plus appendices.

(11) Gross, M. R.; Repka, J.; Robertson, C. T.; Secor, D. H.; Winkle, V. In *W. Sturgeon Conservation: Insights from Elasticity Analysis*, American Fisheries Society Symposium, 2002; Vol. 28, pp 13−30.

(12) Bennett, W. R.; Farrell, A. P. Acute toxicity testing with juvenile white sturgeon (*Acipenser transmontanus*). *Water Qual. Res. J.* **1998**, *33*, 95−110.

(13) Doering, J. A.; Beitel, S. C.; Eisner, B. K.; Heide, T.; Hollert, H.; Giesy, J. P.; Hecker, M.; Wiseman, S. B. Identification and response to metals of metallothionein in two ancient fishes: White sturgeon (*Acipenser transmontanus*) and lake sturgeon (*Acipenser fulvescens*). *Comp. Biochem. Physiol., Part C: Toxicol. Pharmacol.* **2015**, *171*, 41−48.

(14) Vardy, D. W.; Tompsett, A. R.; Sigurdson, J. L.; Doering, J. A.; Zhang, X.; Giesy, J. P.; Hecker, M. Effects of subchronic exposure of early life stages of white sturgeon (*Acipenser transmontanus*) to copper, cadmium, and zinc. *Environ. Toxicol. Chem.* **2011**, *30*, 2497−2505.

(15) Vardy, D. W.; Oellers, J.; Doering, J. A.; Hollert, H.; Giesy, J. P.; Hecker, M. 2013. Sensitivity of early life stages of white sturgeon, rainbow trout, and fathead minnow to copper. *Ecotoxicology* **2013**, *22*, 139−147.

(16) Birstein, V. J. Sturgeons and paddlefishes: threatened fishes in need of conservation. *Conserv. Biol.* **1993**, *7*, 773−787.

(17) Oros, D. R.; Ross, J. R.; Spies, R. B.; Mumley, T. Polycyclic aromatic hydrocarbon (PAH) contamination in San Francisco Bay: a 10-year retrospective of monitoring in an urbanized estuary. *Environ. Res.* **2007**, *105*, 101−118.
(18) Yunker, M. B.; Macdonald, R. W.; Vingarzan, R.; Mitchell, R. H.; Goyette, D.; Sylvestre, S. PAHs in the Fraser River basin: a critical appraisal of PAH ratios as indicators of PAH source and composition. *Org. Geochem.* **2002**, *33*, 489−515.
(19) Doering, J. A.; Wiseman, S.; Beitel, S. C.; Giesy, J. P.; Hecker, M. Identification and expression of aryl hydrocarbon receptors (AhR1 and AhR2) provide insight in an evolutionary context regarding sensitivity of white sturgeon (*Acipenser transmontanus*) to dioxin-like compounds. *Aquat. Toxicol.* **2014**, *150*, 27−35.
(20) Bennett, R. H.; Ellender, B. R.; Mäkinen, T.; Miya, T.; Pattrick, P.; Wasserman, R. J.; Woodford, D. J.; Weyl, O. L. Ethical considerations for field research on fishes. *Koedoe.* **2016**, *58*, No. a1353.
(21) Sloman, K. A.; Bouyoucos, I. A.; Brooks, E. J.; Sneddon, L. U. Ethical considerations in fish research. *J. Fish Biol.* **2019**, *94*, 556−577.
(22) Grech, A.; Brochot, C.; Dorne, J. L.; Quignot, N.; Bois, F. Y.; Beaudouin, R. Toxicokinetic models and related tools in environmental risk assessment of chemicals. *Sci. Total Environ.* **2017**, *578*, 1−15.
(23) Foekema, E. M.; Fischer, A.; Parron, M. L.; Kwadijk, C.; de Vries, P.; Murk, A. J. Toxic concentrations in fish early life stages peak at a critical moment. *Environ. Toxicol. Chem.* **2012**, *31*, 1381−1390.
(24) Grimard, C.; Mangold-Döring, A.; Schmitz, M.; Alharbi, H.; Jones, P. D.; Giesy, J. P.; Hecker, M.; Brinkmann, M. *In vitro*-in vivo and cross-life stage extrapolation of uptake and biotransformation of benzo[*a*]pyrene in the fathead minnow (*Pimephales promelas*). *Aquat. Toxicol.* **2020**, No. 105616.
(25) Nichols, J. W.; McKim, J. M.; Andersen, M. E.; Gargas, M. L.; Clewell, H. J.; Erickson, R. J. A physiologically based toxicokinetic model for the uptake and disposition of waterborne organic chemicals in fish. *Toxicol. Appl. Pharmacol.* **1990**, *106*, 433−447.
(26) Stadnicka, J.; Schirmer, K.; Ashauer, R. Predicting concentrations of organic chemicals in fish by using toxicokinetic models. *Environ. Sci. Technol.* **2012**, *46*, 3273−3280.
(27) Nichols, J. W.; Fitzsimmons, P. N.; Burkhard, L. P. In vitro-in vivo extrapolation of quantitative hepatic biotransformation data for fish. II. Modeled effects on chemical bioaccumulation. *Environ. Toxicol. Chem.* **2007**, *26*, 1304−1319.
(28) Nichols, J. W.; Hoffman, A. D.; ter Laak, T. L.; Fitzsimmons, P. N. Hepatic clearance of 6 polycyclic aromatic hydrocarbons by isolated perfused trout livers: prediction from in vitro clearance by liver S9 fractions. *Toxicol. Sci.* **2013**, *136*, 359−372.
(29) Tompsett, A. R.; Vardy, D. W.; Higley, E.; Doering, J. A.; Allan, M.; Liber, K.; Giesy, J. P.; Hecker, M. Effects of Columbia River water on early life-stages of white sturgeon (*Acipenser transmontanus*). *Ecotoxicol. Environ. Saf.* **2014**, *101*, 23−30.
(30) Arnot, J. A.; Gobas, F. A. A food web bioaccumulation model for organic chemicals in aquatic ecosystems. *Environ. Toxicol. Chem.* **2004**, *23*, 2343−2355.
(31) Brinkmann, M.; Schlechtriem, C.; Reininghaus, M.; Eichbaum, K.; Buchinger, S.; Reifferscheid, G.; Hollert, H.; Preuss, T. G. Cross-species extrapolation of uptake and disposition of neutral organic chemicals in fish using a multispecies physiologically-based toxicokinetic model framework. *Environ Sci. Technol.* **2016**, *50*, 1914−1923.
(32) U.S. Environmental Protection Agency (EPA). (2006) Approaches for the Application of Physiologically Based Pharmacokinetic (PBPK) Models and Supporting Data in Risk Assessment. National Center for Environmental Assessment, Washington, DC; EPA/600/R-05/043F. Available from: National Technical Information Service, Springfield, VA, and online at http://epa.gov/ncea.
(33) Chiu, W.; Barton, H.; DeWoskin, R.; Schlosser, P.; Thompson, C.; Sonawane, B.; Lipscomb, J. C.; Krishnan, K. Evaluation of physiologically based pharmacokinetic models for use in risk assessment. *J. Appl. Toxicol.* **2007**, *27*, 218−237.
(34) OECD. Test No. 319B: Determination of in vitro intrinsic clearance using rainbow trout liver S9 sub-cellular fraction (RT-S9). *OECD Guidelines for the Testing of Chemicals* 2018, Section 3, OECD Publishing: Paris.
(35) Kennedy, S. W.; Jones, S. P. Simultaneous measurement of cytochrome P4501A catalytic activity and total protein concentration with a fluorescence plate reader. *Anal. Biochem.* **1994**, *222*, 217−223.
(36) Habig, W. H.; Pabst, M. J.; Jakoby, W. B. Glutathione S-transferases the first enzymatic step in mercapturic acid formation. *J. Biol. Chem.* **1974**, *249*, 7130−7139.
(37) Eichelberger, J. W.; Behymer, T. D.; Budde, W. L. *Determination of Organic Compounds in Drinking Water by Liquid-solid Extraction and Capillary Column Gas Chromatography/mass Spectrometry: Test Method 525.1*; US Environmental Protection Agency, 1988.
(38) Lu, Y.; Ludsin, S. A.; Fanslow, D. L.; Pothoven, S. A. Comparison of three microquantity techniques for measuring total lipids in fish. *Can. J. Fish. Aquat. Sci.* **2008**, *65*, 2233−2241.
(39) Le Fol, V.; Brion, F.; Hillenweck, A.; Perdu, E.; Bruel, S.; Aït-Aïssa, S.; Cravedi, J.-P.; Zalko, D. Comparison of the in vivo biotransformation of two emerging estrogenic contaminants, BP2 and BPS, in zebrafish embryos and adults. *Int. J. Mol. Sci.* **2017**, *18*, No. 704.
(40) Pettem, C. M.; Briens, J. M.; Janz, D. M.; Weber, L. P. Cardiometabolic response of juvenile rainbow trout exposed to dietary selenomethionine. *Aquat. Toxicol.* **2018**, *198*, 175−189.
(41) Froese, R.; Pauly, D.. *FishBase. World Wide Web electronic publication*, version (12/2019). www.fishbase.org, 2019.
(42) Shen, J.; Zhang, Q.; Ding, S.; Zhang, S.; Coats, J. R. Bioconcentration and elimination of avermectin B1 in sturgeon. *Environ. Toxicol. Chem.* **2005**, *24*, 396−399.
(43) Tjeerdema, R. S.; Crosby, D. G. Comparative biotransformation of molinate (Ordram) in the white sturgeon (*Acipenser transmontanus*) and common carp (*Cyprinus carpio*). *Xenobiotica* **1988**, *18*, 831−838.
(44) Hou, X.; Shen, J.; Zhang, S.; Jiang, H.; Coats, J. R. Bioconcentration and elimination of sulfamethazine and its main metabolite in sturgeon (*Acipenser schrenkii*). *J. Agric. Food Chem.* **2003**, *51*, 7725−7729.
(45) TenBrook, P. L.; Kendall, S. M.; Tjeerdema, R. S. Toxicokinetics and biotransformation of p-nitrophenol in white sturgeon (*Acipenser transmontanus*). *Ecotoxicol. Environ. Saf.* **2006**, *64*, 362−368.
(46) Gelboin, H. V. Benzo[*a*]pyrene metabolism, activation, and carcinogenesis: Role and regulation of mixed-function oxidases and related enzymes. *Physiol. Rev.* **1980**, *60*, 1107−1166.
(47) McKim, J.; Schmieder, P.; Veith, G. Absorption dynamics of organic chemical transport across trout gills as related to octanol-water partition coefficient. *Toxicol. Appl. Pharmacol.* **1985**, *77*, 1−10.
(48) McKim, J. M.; Erickson, R. J. Environmental impacts on the physiological mechanisms controlling xenobiotic transfer across fish gills. *Physiol. Zool.* **1991**, *64*, 39−67.
(49) Bertelsen, S. L.; Hoffman, A. D.; Gallinat, C. A.; Elonen, C. M.; Nichols, J. W. Evaluation of log Kow and tissue lipid content as predictors of chemical partitioning to fish tissues. *Environ. Toxicol. Chem.* **1998**, *17*, 1447−1455.
(50) Liu, F.; Wiseman, S.; Wan, Y.; Doering, J. A.; Hecker, M.; Lam, M. H.; Giesy, J. P. Multi-species comparison of the mechanism of biotransformation of MeO-BDEs to OH-BDEs in fish. *Aquat. Toxicol.* **2012**, *114*−*115*, 182−188.
(51) Jönsson, M. E.; Jenny, M. J.; Woodin, B. R.; Hahn, M. E.; Stegeman, J. J. Role of AHR2 in the expression of novel cytochrome P450 1 family genes, cell cycle genes, and morphological defects in developing zebra fish exposed to 3, 3′, 4, 4′, 5-pentachlorobiphenyl or 2, 3, 7, 8-tetrachlorodibenzo-p-dioxin. *Toxicol. Sci.* **2007**, *100*, 180−193.
(52) Schiwy, S.; Br unig, J.; Alert, H.; Hollert, H.; Keiter, S. H. A novel contact assay for testing aryl hydrocarbon receptor (AhR)-mediated toxicity of chemicals and whole sediments in zebrafish

https://doi.org/10.1021/acs.est.0c06867
Environ. Sci. Technol. 2021, 55, 11590−11600

(*Danio rerio*) embryos. *Environ. Sci. Pollut. Res.* **2015**, *22*, 16305−16318.
(53) Wang, L.; Camus, A. C.; Dong, W.; Thornton, C.; Willett, K. L. Expression of CYP1C1 and CYP1A in Fundulus heteroclitus during PAH-induced carcinogenesis. *Aquat. Toxicol.* **2010**, *99*, 439−447.
(54) Yuan, L.; Lv, B.; Zha, J.; Wang, Z. Benzo [*a*] pyrene induced p53-mediated cell cycle arrest, DNA repair, and apoptosis pathways in Chinese rare minnow (*Gobiocypris rarus*). *Environ. Toxicol.* **2017**, *32*, 979−988.
(55) van der Heijden, S. A.; Hermens, J. L.; Sinnige, T. L.; Mayer, P.; Gilbert, D.; Jonker, M. T. Determining high-quality critical body residues for multiple species and chemicals by applying improved experimental design and data interpretation concepts. *Environ. Sci. Technol.* **2015**, *49*, 1879−1887.
(56) Otte, J. C.; Schmidt, A. D.; Hollert, H.; Braunbeck, T. Spatio-temporal development of CYP1 activity in early life-stages of zebrafish (*Danio rerio*). *Aquat. Toxicol.* **2010**, *100*, 38−50.
(57) Wan, Y.; Wei, Q.; Hu, J.; Jin, X.; Zhang, Z.; Zhen, H.; Liu, J. Levels, tissue distribution, and age-related accumulation of synthetic musk fragrances in Chinese sturgeon (*Acipenser sinensis*): Comparison to organochlorines. *Environ. Sci. Technol.* **2007**, *41*, 424−430.
(58) Zhang, K.; Wan, Y.; Giesy, J. P.; Lam, M. H.; Wiseman, S.; Jones, P. D.; Hu, J. Tissue concentrations of polybrominated compounds in Chinese sturgeon (*Acipenser sinensis*): origin, hepatic sequestration, and maternal transfer. *Environ. Sci. Technol.* **2010**, *44*, 5781−5786.
(59) Lam, S. H.; Ung, C. Y.; Hlaing, M. M.; Hu, J.; Li, Z. H.; Mathavan, S.; Gong, Z. Molecular insights into 4-nitrophenol-induced hepatotoxicity in zebrafish: Transcriptomic, histological and targeted gene expression analyses. *Biochim. Biophys. Acta, Gen. Subj.* **2013**, *1830*, 4778−4789.
(60) Cochran, R. C.; Formoli, T. A.; Pfeifer, K. F.; Aldous, C. N. Characterization of risks associated with the use of molinate. *Regul. Toxicol. Pharmacol.* **1997**, *25*, 146−157.
(61) Tjeerdema, R. S.; Crosby, D. G. The biotransformation of molinate (Ordram) in the striped bass (*Morone saxatilis*). *Aquat. Toxicol.* **1987**, *9*, 305−317.
(62) Tjeerdema, R. S.; Crosby, D. G. Disposition, biotransformation, and detoxication of molinate (Ordram) in whole blood of the common carp (*Cyprinus carpio*). *Pesticic. Biochem. Physiol.* **1988**, *31*, 24−35.
(63) Halley, B. A.; VandenHeuvel, W. J.; Wislocki, P. G. Environmental effects of the usage of avermectins in livestock. *Vet. Parasitol.* **1993**, *48*, 109−125.
(64) Van den Heuvel, W. J. A.; Halley, B. A.; Ku, C. C.; Jacob, T. A.; Wislocki, P. G.; Forbis, A. D. Bioconcentration and depuration of avermectin B1a in the bluegill sunfish. *Environ. Toxicol. Chem.* **1996**, *15*, 2263−2266.
(65) Spacie, A.; Hamelink, J. L. Alternative models for describing the bioconcentration of organics in fish. *Environ. Toxicol. Chem.* **1982**, *1*, 309−320.
(66) Gobas, F. A.; Opperhuizen, A.; Hutzinger, O. Bioconcentration of hydrophobic chemicals in fish: relationship with membrane permeation. *Environ. Toxicol. Chem.* **1986**, *5*, 637−646.
(67) Guo, X.; Peng, Z.; Huang, D.; Xu, P.; Zeng, G.; Zhou, S.; Luo, H.; et al. Biotransformation of cadmium-sulfamethazine combined pollutant in aqueous environments: Phanerochaete chrysosporium bring cautious optimism. *Chem. Eng. J.* **2018**, *347*, 74−83.
(68) Ji, K.; Kim, S.; Han, S.; Seo, J.; Lee, S.; Park, Y.; Choi, K.; et al. Risk assessment of chlortetracycline, oxytetracycline, sulfamethazine, sulfathiazole, and erythromycin in aquatic environment: are the current environmental concentrations safe? *Ecotoxicology* **2012**, *21*, 2031−2050.
(69) Ramesh, M.; Thilagavathi, T.; Rathika, R.; Poopal, R. K. Antioxidant status, biochemical, and hematological responses in a cultivable fish Cirrhinus mrigala exposed to an aquaculture antibiotic Sulfamethazine. *Aquaculture* **2018**, *491*, 10−19.
(70) Chen, Y.; Hermens, J. L.; Jonker, M. T.; Arnot, J. A.; Armitage, J. M.; Brown, T.; Droge, S. T.; et al. Which molecular features affect the intrinsic hepatic clearance rate of ionizable organic chemicals in fish? *Environ. Sci. Technol.* **2016**, *50*, 12722−12731.
(71) Fay, K. A.; Fitzsimmons, P. N.; Hoffman, A. D.; Nichols, J. W. Comparison of trout hepatocytes and liver S9 fractions as in vitro models for predicting hepatic clearance in fish. *Environ. Toxicol. Chem.* **2017**, *36*, 463−471.
(72) Nichols, J. W.; Huggett, D. B.; Arnot, J. A.; Fitzsimmons, P. N.; Cowan-Ellsberry, C. E. Toward improved models for predicting bioconcentration of well-metabolized compounds by rainbow trout using measured rates of in vitro intrinsic clearance. *Environ. Toxicol. Chem.* **2013**, *32*, 1611−1622.
(73) Wang, H.; Xia, X.; Liu, R.; Wang, Z.; Lin, X.; Muir, D. C.; Wang, W. X. Multicompartmental toxicokinetic modeling of discrete dietary and continuous waterborne uptake of two polycyclic aromatic hydrocarbons by zebrafish *Danio rerio*. *Environ. Sci. Technol.* **2020**, *54*, 1054−1065.
(74) Wang, H.; Xia, X.; Wang, Z.; Liu, R.; Muir, D. C.; Wang, W. X. Contribution of Dietary Uptake to PAH Bioaccumulation in a Simplified Pelagic Food Chain: Modeling the Influences of Continuous vs Intermittent Feeding in Zooplankton and Fish. *Environ. Sci. Technol.* **2021**, *55*, 1930−1940.

https://doi.org/10.1021/acs.est.0c06867
Environ. Sci. Technol. 2021, 55, 11590−11600

SUPPLEMENTARY INFORMATION

Toxicokinetic models for bioconcentration of organic contaminants in two life stages of white sturgeon (*Acipenser transmontanus*)

Chelsea Grimard, Annika Mangold-Döring, Hattan Alharbi, Lynn Weber, Natacha Hogan, Paul D. Jones, John P. Giesy, Markus Hecker, Markus Brinkmann

Total page number: 35, including 4 tables and 10 figures

1. Study design

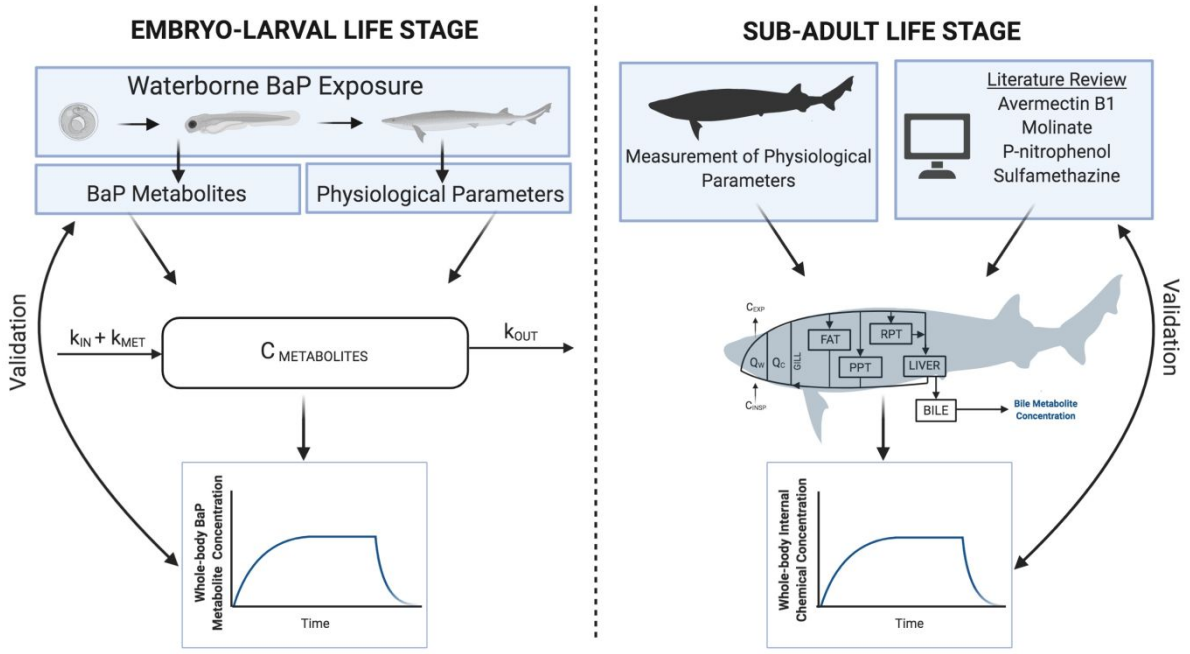

Figure S1. Conceptual flow chart of the study design. BaP = benzo[*a*]pyrene; $C_{METABOLITES}$ = whole-body metabolite concentration; k_{IN} = uptake rate constant, k_{MET} = whole body biotransformation rate constant; k_{OUT} = elimination rate constant; PPT = poorly perfused tissues, RPT = richly perfused tissues.

2. Embryo-larval waterborne B[*a*]P exposure

A chronic waterborne B[*a*]P exposure was conducted for 49 days to evaluate the uptake and biotransformation of B[*a*]P during the egg, yolk, and free-feeding developmental stages of the white sturgeon. Embryos (<24 hours post-fertilization) were initially exposed in glass jars containing facility water from the supplier spiked with B[*a*]P (CAS 50-32-8, Sigma-Aldrich, Oakville, ON, CAN) to obtain nominal concentrations of 1.3, 4.0 and 12.0 µg B[*a*]P/L using 0.02% DMSO (≥ 99.9% dimethyl sulfoxide, Fisher Scientific Co., Ottawa, ON, CAN) as the solvent carrier, or 0.02% DMSO only as the solvent control, or facility water as the water control (*n*=4 per treatment). Five days post fertilization (dpf), the exposed embryos were transported to the Aquatic Toxicology Research Facility (ATRF) at the University of Saskatchewan and the jars were placed into 7-L aquaria containing 50% reverse osmosis water,

50% ATRF facility water as water bath which maintained a temperature of 14°C ± 1°C. At hatch, the embryos within the jars were carefully emptied into the aquaria for the remainder of exposure. After 49 days of exposure, three remaining larvae (*n*=4 per treatment) underwent a seven-day depuration period in which all tanks were switched to clean water. A 50% daily static renewal system was maintained throughout all phases of exposure. The larvae were fed a diet of one or two-day-old *Artemia spp.* nauplii three times daily *ad libitum* starting prior to swim-up, i.e., ~10 days post-hatch.

Water quality parameters temperature (°C), dissolved oxygen (%), pH, conductivity (μS/cm), ammonia (mg/L), nitrates (mg/L), nitrites (mg/L), hardness (mg/L), and alkalinity (mg/L) were recorded from a random distribution of tanks weekly. Temperature, dissolved oxygen, pH, and conductivity were measured using a hand-held digital instrument (YSI Professional Plus, YSI Inc.). Nitrates and nitrites were measured using colorimetric kits, and hardness and alkalinity were measured using titrations kits from LaMotte Co. (Chestertown, MD, USA). Ammonia was measured using the colorimetric API ammonia test kit (Mars Fishcare).

3. Determination of EROD activity

7-ethoxyresorufin *O*-deethylase (EROD) activity was measured in triplicates following the protocol previously described by Kennedy & Jones,[1] with modifications. The protocol is also described by Grimard et al.[8] for fathead minnow larvae. The reagents bovine serum albumin (BSA, CAS 9048-46-8), Ethylenediaminetetraacetic acid (EDTA, CAS 6381-92-6), DL-dithiothreitol (DTT, CAS 3483-12-3), fluorescamine (CAS 38183-12-9), HEPES (CAS 7365-45-9), potassium chloride (KCl, CAS 7447-40-7), nicotinamide adenine dinucleotide phosphate reduced (NADPH, CAS 100929-71-3), resorufin (CAS 653-78-9), sucrose (CAS 57-50-1), and Tris-HCl (Trizma®Base, CAS 77-86-1) were purchased from Sigma-Aldrich (Oakville, ON, CAN), and ethoxyresorufin (CAS 5725-91-7) was purchased from Fisher Scientific Co.

(Ottawa, ON, CAN). Following a modified protocol of what is described by OECD 319B[2], the post-mitochondrial supernatant fraction was generated from seven, 21, and 42 dpf whole-body larval white sturgeon. One larval fish (*n*=3 per treatment) was homogenized on ice in homogenization buffer (150 mM Tris-HCl, 150 mM KCl, 2 mM EDTA, 1 mM DTT, 250 mM sucrose) at a ratio of 20 µL buffer: 1 mg tissue. The homogenate was subsequently centrifuged at 10,000xg and the supernatant was sampled for use in subsequent biochemical assays. HEPES buffer (0.05 M, pH 7.8), BSA (2 mg/mL in HEPES), and resorufin (1.9 µM in HEPES) was added to six sets of triplicate wells of a 96 well plate to produce a six-point resorufin (0, 1.9, 3.8, 7.5, 15, 60 µM) and protein (0, 0.006, 0.012, 0.024, 0.036, 0.48 µM) standard curve. The supernatant (12 µL) for each sample was added to separate triplicate wells, and to an additional single well to act as a sample blank. Ethoxyresorufin (250 µM in HEPES; 30 µL) was added to all used wells and the plate was incubated at room temperature, in darkness, for 10 minutes. To initiate the reaction, NADPH (0.3 mM in HEPES, 30 µL) was added to all wells, except the sample blanks. The plate was subsequently incubated at 25°C in darkness for 30 minutes. Fluorescamine in ACN (600 µg/mL; 60 µL) was added to all used wells to stop the reaction and the plate underwent an additional incubation period of 15 minutes at room temperature in darkness. Using a multi-well plate reader (POLARstar Optima, BMG Labtech, Ortenberg, Germany), fluorescence of resorufin was read at 570 nm excitation/ 630 nm emission and proteins at 365 nm excitation/ 480 nm emission. EROD activity results, specific to the embryo-larval white sturgeon exposure, are shown in Figure S2.

4. Determination of GST activity

Glutathione *S*-transferase (GST) activity was measured in triplicates following the protocol described by Habig et al.,[3] adapted to microplates. Grimard et al.[8] also described the protocol in regard to fathead minnow larvae. 1-Chloro-2,4-dinitrobenzene (CDNB, CAS 97-00-7), glutathione reduced (GSH, CAS 70-18-8), and potassium phosphate were purchased from

Sigma-Aldrich. The post-mitochondrial supernatant fraction was produced as described for the EROD assay. Active wells were produced by adding phosphate buffer (0.1 M, pH 6.5, 250 µL) to triplicate wells and sample blanks were produced by adding phosphate buffer (0.1 M, pH 6.5, 275 µL) to an individual well. The post-mitochondrial supernatant (20 µL) and CDNB (25 mM in ethanol; 10 µL) were added to all used wells. An additional well (homogenization blank) containing phosphate buffer (0.1 M, pH 6.5, 250 µL), homogenization buffer (25 µL) and CDNB (25 mM in ethanol; 10 µL was produced to account for spontaneous reaction with the homogenization buffer. To initiate the reaction, GSH (11.4 mM in phosphate buffer; 25 µL) was added to all active wells and the homogenization blank. Using a multi-well plate reader (POLARstar Optima, BMG Labtech), a kinetic absorbance reading (340 nm) was immediately started and run for 10 minutes at 25°C. The concentration of CDNB was calculated using the Lambert-beer law. The molar extinction coefficient of 9.6 1/(mM cm) was used to calculate GST activity (nmol CDNB/mg protein/min). The protein concentration of the S9 was measured using the BCA (bicinchoninic acid) protein assay kit (Sigma-Aldrich). GST activity results, specific to the embryo-larval white sturgeon exposure, are shown in Figure S3.

5. Measurement of intrinsic clearance

Intrinsic clearance was measured in triplicates following the protocol described in OECD319b,[2] with modifications. The protocol is also described by Grimard et al.[8] for adult fathead minnow. Adenosine triphosphate (ATP, CAS 34369-07-8), Nicotinamide adenine dinucleotide phosphate reduced (NADPH, CAS 100929-71-3), glucose-6-phosphate (G6P, CAS 54010-71-8), glutathione reduced (GSH, CAS 70-18-8), and uridine 5'-diphosphoglucuronic acid (UDPGA, CAS 63700-19-6) were purchased from Sigma-Aldrich. Three replicates of three pooled white sturgeon livers were used to obtain the post mitochondrial supernatant (S9) fraction. To generate the supernatant (S9), pooled liver tissue was homogenized in 3 µL homogenization buffer: 1 mg tissue. The homogenate was subsequently centrifuged at 9,000xg

for 20 minutes. The supernatant (S9) was sampled for use in the *in vitro* clearance assay, and the protein concentration of the S9 was determined using the BCA (bicinchoninic acid) protein assay. A co-substrate mixture described by Richardson et al.[4] was generated, with modifications, using ATP (11.1 mM), G6P (5.55 mM), GSH (2.77 mM), NADPH (0.55mM), and UDPGA (0.55mM) reconstituted in phosphate buffer (pH 7.4; 100 mM potassium phosphate, 5 mM magnesium chloride, 5 mM magnesium sulfate), to create a PAPS (3'-phosphoadenosine-5'-phosphosulfate) regenerating system. The S9 was diluted to a protein concentration of 10 mg/L. Diluted S9 (100 µL) and the co-substrates (900 µL) were combined in a glass cell culture tube. The total protein concentration of the reaction mixture was 1 mg/L. The solution was spiked with 250µM B[*a*]P in ACN to obtain a concentration of 0.5 µM B[*a*]P. The solution was immediately incubated along side a blank, that only contained the co-substrates and B[*a*]P, at 25°C in a shaking incubator (New Brunswick™, Innova 40®). Sub-samples of the solution were taken after 0, 30, 60, 90, 120, 180, and 240 minutes, and quenched in ice-cold ACN, and centrifuged at 1700×g for 15 minutes. Parent B[*a*]P concentrations were subsequently analyzed using synchronous fluorescence spectrophotometry in a quartz cuvette (Lumina, Thermo Fisher Scientific, Ottawa, ON, CAN). Parent B[*a*]P signaled between 400-440 nm and the B[*a*]P metabolites between 420-480 nm. Each metabolite was measured and validated using neat B[*a*]P and OH-B[*a*]P standards. Using a 6-point standard curve (0.00, 0.03, 0.06, 0.13, 0.25, and 0.50 µM) the peak area of the B[*a*]P curve was interpolated for each time point. The concentrations were plotted against time to generate a depletion curve which was subsequently *log*-transformed. The slope was determined by subtracting the slope of the blank curve from the slope of the reaction curve. The first-order depletion rate constant (*k*) was determined by multiplying the average slope of the line between all three replicates (-0.09522 h^{-1}; Figure S5) by -2.3. Intrinsic clearance ($Cl_{int,\ in\ vitro}$) was calculated as (Eq. S1):

$$Cl_{int,\ in\ vitro}(mL\ h^{-1}mg^{-1}) = \frac{k(h^{-1}) \cdot volume\ of\ the\ reaction\ (mL)}{reaction\ protein\ concentration\ (mg\ L^{-1})} \qquad (S1)$$

Sub-adult *in vitro* intrinsic clearance depletion curves are presented in Figure S5. The value for white sturgeon sub-adult *in vitro* clearance was calculated to be 0.219 mL h^{-1} mg^{-1}.

6. Lipid analysis

Total whole-body lipid content in both life stages of white sturgeon was quantified using a modification of the microcolorimetric sulfophosphovanillin (SPV) described by Lu et al.[5] Grimard et al.[8] also described the protocol for whole body adult and larval fathead minnow. The reagents sulphuric acid (CAS 7664-93-9) and phosphoric acid (CAS 7664-38-2) were purchased from Thermo Fisher Scientific. Vanillin (CAS 48-53-8) was purchased from Sigma-Aldrich. Lipids were extracted using triplicate samples of whole-body embryo-larval fish (30-120 mg wet weight) or homogenized sub-samples of adult tissues (20-100mg sub-sample; liver, kidney, spleen, muscle, brain, gills, viscera, and carcass). The samples were homogenized in a 2:1 mixture (v/v) of chloroform and methanol followed by saline (200µl) for lipid purification. Extra chloroform: methanol (200 µL) was added for samples in which sample weight exceeded 50 mg to ensure complete homogenization of the sample and appropriate lipid concentrations. In 5-mL glass culture tubes, the lipid extracts (200 µL) were evaporated using a dry bath heater. Sulphuric acid (62.5 µL) and SPV reagent (1.25 mL of a solution containing 0.75 g vanillin in 0.125 L deionized water and 0.5 L phosphoric acid) were added to the evaporated lipid samples. A 6-point standard curve (0.00, 0.16, 0.31, 0.63, 1.25, 5.00 mg/mL) was developed from a serial dilution of cod liver oil (CAS 8001-69-2, Sigma Aldrich) in 2:1 (v/v) chloroform:methanol. The samples and standard curve were added to a 96-well plate and a multi-well plate reader (POLARstar Optima, BMG Labtech, Ortenberg, Germany) was used to measure absorbance at 525nm. Lipid content of the samples was interpolated using the standard curve.

7. One-compartment embryo-larval life stage model

The one-compartment bioaccumulation model described by Arnot and Gobas[6] (Table S2) was adapted to predict the abundance of parent B[*a*]P and B[*a*]P metabolites in the ELS (embryo-larval stage) of white sturgeon exposed aqueously to B[*a*]P. Biotransformation of B[*a*]P was integrated into the model through a whole-body biotransformation rate constant (k_{MET}). Because embryo-larval biotransformation could not be appropriately measured or scaled from sub-adult white sturgeon *in vitro* clearance (Figure S6), k_{MET} was calibrated using a training data set consisting of 21 randomly selected data points out of the 42 measured values of B[*a*]P metabolite abundances. The k_{MET} values were obtained by adjusting *in vitro* clearance, in an allometric scaling equation (Table S1) that uses estimates of cardiac output. Predictions tested with the k_{MET} values calculated using the *in vitro* clearance value set at the lowest observable detection (LOD) value and half the LOD from the OECD 319B intrinsic clearance assay[2] are shown in Figure S7 and S8, respectively. Values between 50- and 300-fold lower than the measured sub-adult white sturgeon *in vitro* clearance were also tested. An *in vitro* clearance value 280-fold lower (0.00078 mL h^{-1} mg^{-1}) than the measured sub-adult white sturgeon *in vitro* clearance was determined to be the most appropriate value for use in the model to generate the highest achievable number of predictions within one order of magnitude of the training set of measured values (Figure S9).

The model was implemented using Python 3.5® (Python Software Foundation, Wilmington, DE, USA) in Jupyter Notebook® (Project Jupyter, U.S. Patent & Trademark Office, Alexandria, VA, USA). A series of matrices were used for the parameters wet weight (w_w), whole-body lipid content (lipid) and the whole body biotransformation rate constant (k_met) to describe the time function of parameters, i.e., the relationship between the parameter value and life stage (i.e., 0, 7, 12, 21, 35, 42, 49, or 56 days post fertilization (dpf)). A simulated exposure was run at the three measured average exposure concentrations, 2.08, 4.11, and 9.11 µg B[*a*]P/L for 49 days, 1000 iteration steps per day. The accumulation of B[*a*]P

metabolites were predicted in the whole-body white sturgeon larvae using the model (Figure S4).

Supplemental Table S1. Spreadsheet inputs and parameters for the embryo-larval life stage of white sturgeon (*Acipenser transmontanus)* to calculate whole-body metabolism rate. The table is based on Nichols et al.[7]

Symbol	Units	Description	Value						
			Egg stage (0-12 dpf)	Yolk stage (12-21 dpf)		Free feeding stage (21-56 dpf)			
			7 dpf	12 dpf	21 dpf	35 dpf	42 dpf	49 dpf	56 dpf
Rate	h^{-1}	Depletion rate constant[a]	0.00078[a]						
Bwg	g	Fish wet weight	0.04911	0.03230	0.04009	0.04938	0.05950	0.08260	0.1242
log K_{ow}	-	Octanol-water partitioning coefficient	6.19						
C_{S9}	mg mL^{-1}	S9 protein concentration	– Adult value assumed (Supplemental Table S3) –						
L_{S9}	mg g $liver^{-1}$	Total liver S9 protein content	– Adult value assumed (Supplemental Table S3) –						
L_{FBW}	g liver g wet $weight^{-1}$	Fractional liver weight	– Adult value assumed (Supplemental Table S3) –						
V_{LWB}	-	Fractional whole-body lipid content	0.0285	0.0362	0.0299	0.0254	0.0138	0.0047	0.0025
Q_C	L d^{-1} kg^{-1}	Cardiac output[b]	34.980[b]	34.980[b]	110.868[b]	39.528[b]	39.528[b]	39.528[b]	39.528[b]
Q_{HFRAC}	-	Liver blood flow as a fraction of cardiac output	– Adult value assumed (Supplemental Table S3) –						
V_{WBL}	-	Fractional blood water content	– Adult value assumed (Supplemental Table S3) –						
f_u	-	Binding correction term	1.0 (assumed)						
$CL_{IN\ VITRO,INT}$	mL h^{-1} mg S9 $protein^{-1}$	*In vitro* intrinsic clearance	– Equation S2 –						

$CL_{IN\ VIVO,INT}$	L d^{-1} kg^{-1}	*In vivo* intrinsic clearance	– Equation S3 –
Q_H	L d^{-1} kg^{-1}	Liver blood flow	– Equation S4–
Cl_H	L d^{-1} kg^{-1}	Hepatic clearance	– Equation S5 –
P_{bw}	-	Blood:water partitioning coefficient	– Equation S6 –
BCF_P	L kg^{-1}	Partitioning based BCF	– Equation S7 –
$V_{D,BL}$	L kg^{-1}	Volume of distribution to blood plasma	– Equation S8 –
k_{met}	d^{-1}	Whole-body biotransformation rate	– Equation S9 –

[a]*calibrated to produce k_{MET} values that resulted in the greatest achievable number of predictions to be within 10-fold of the training set of measured values*

[b]*stage-matched and assumed to be equivalent to cardiac output measured in fathead minnow larvae (Grimard et al.*[8])

Spreadsheet equations for calculation of k_{met} (Nichols et al.[7])

In vitro intrinsic clearance

$$Cl_{in\ vitro,\ int} = \frac{rate}{C_{s9}}\ ;\ (\text{mL h}^{-1}\ \text{mg S9 protein}^{-1}) \qquad \textbf{(Eq. S2)}$$

In vivo intrinsic clearance

$$CL_{in\ vivo,\ int} = CL_{in\ vitro,int} \cdot L_{S9} \cdot L_{FBW} \cdot 24h\ ;\ (\text{L d}^{-1}\ \text{kg}^{-1}) \qquad \textbf{(Eq. S3)}$$

Liver blood flow

$$Q_H = Q_C \cdot Q_{HFRAC}\ ;\ (\text{L d}^{-1}\ \text{kg}^{-1}) \qquad \textbf{(Eq. S4)}$$

Hepatic clearance

$$CL_H = \frac{Q_H \cdot f_u \cdot CL_{in\ vivo,int}}{Q_H + f_u \cdot CL_{in\ vivo,int}}\ ;\ (\text{L d}^{-1}\ \text{kg}^{-1}) \qquad \textbf{(Eq. S5)}$$

Blood:water partition coefficient

$$P_{bw} = 10^{0.73 \cdot log\ K_{ow}} \cdot 0.16 + V_{WBL}\ ;\ (\text{unitless}) \qquad \textbf{(Eq. S6)}$$

Partitioning based bioaccumulation factor

$$BCF_P = V_{LWB} \cdot 10^{log\ k_{ow}}\ ;\ (\text{L kg}^{-1}) \qquad \textbf{(Eq. S7)}$$

Volume of distribution to blood plasma

$$V_{D,BL} = \frac{BCF_P}{P_{BW}}\ ;\ (\text{L kg}^{-1}) \qquad \textbf{(Eq. S8)}$$

Whole body metabolism rate

$$k_{met} = \frac{CL_H}{V_{D,BL}}\ ;\ (\text{d}^{-1}) \qquad \textbf{(Eq. S9)}$$

Supplemental Table S2. Model inputs and parameters of the one-compartment model for the embryo-larval life stage of white sturgeon (*Acipenser transmontanus*). The table is based on Arnot and Gobas[6]. The compartment is assumed to have a specific gravity of 1.0 (i.e. the units L and kg can be substitute for another).

Symbol	Units	Description	Value		
			Egg stage (0-12 dpf)	Yolk stage (12-21 dpf)	Free feeding stage (21-56 dpf)
w_w	kg (L)	Body wet mass (volume of the whole body)	– Model input –		
K_{ow}	-	Octanol-water partitioning coefficient	– Model input –		
S	%	Dissolved oxygen saturation	– Model input –		
T	°C	Water temperature	– Model input –		
C_w	µg L^{-1}	Chemical concentration in water	– Model input –		
f_lipid	%	Total lipid content (fraction of body weight)	– Model input –		
lipid	kg	Total lipid content	– Equation S10 –		
β	-	Sorption capacity constant	0.05*	0.05*	0.05*
d_w	kg	Body dry mass	0.28 w_w		
f_NLOM	-	Fraction of non-lipid organic matter	– Equation S11 –		
f_water	-	Water content	– Equation S12 –		
K_{bw}	-	Fish – water partition coefficient	– Equation S13 –		
C_{ox}	mg O_2 L^{-1}	Dissolved oxygen concentration in water	– Equation S14 –		
G_v	L d^{-1}	Gill ventilation rate	– Equation S15–		
E_w	-	Gill chemical uptake efficiency	– Equation S16 –		

k_{in}	L kg^{-1} d^{-1}	Aqueous uptake clearance rate constant	– Equation S17 –
k_{out}	kg kg^{-1} d^{-1}	Gill elimination rate constant	– Equation S18 –
k_G	d^{-1}	Growth dilution rate constant	– Equation S19 –
k_{met}	d^{-1}	Whole-body metabolism rate	– Equation S9 –
C_{int}	µg g^{-1}	Chemical internal concentration (excluding metabolism)	– Equation S20 –
C_{met}	µg g^{-1}	Metabolite internal concentration	– Equation S21 –

[*] *Value is different than what is reported by Arnot & Gobas[6]. Value obtained from DeBruyn & Gobas[9] as suggested by Stadnicka et al.[10].*

Embryo-larval stage one-compartment model equations (from Arnot and Gobas[6])

Total lipid content

$$lipid = w\_w \cdot f\_lipid \text{ ; (kg)} \quad \textbf{(Eq. S10)}$$

Fraction of non-lipid organic matter

$$f\_NLOM = \frac{d\_w - lipid}{w\_w} \text{ ; (unitless)} \quad \textbf{(Eq. S11)}$$

Water fraction in fish

$$f\_water = \frac{w\_w - d\_w}{w\_w} \text{ ; (unitless)} \quad \textbf{(Eq. S12)}$$

Fish – water partition coefficient

$$k_{bw} = f\_lipid \cdot K_{ow} + f\_NLOM \cdot \beta \cdot K_{OW} + f\_water \text{ ; (unitless)} \quad \textbf{(Eq. S13)}$$

Dissolved oxygen concentration

$$C_{ox} = (-0.24 \cdot T + 14.04) \cdot \frac{S}{100} \text{ ; (mg } O_2 \text{ } L^{-1}) \quad \textbf{(Eq. S14)}$$

Gill ventilation rate

$$G_v = 1400 \cdot \frac{w\_w^{0.65}}{C_{ox}} \text{ ; (L } d^{-1}) \quad \textbf{(Eq. S15)}$$

Gill chemical uptake efficiency

$$E_w = \frac{1}{1.85 + \frac{155}{K_{ow}}} \text{ ; (unitless)} \quad \textbf{(Eq. S16)}$$

Aqueous uptake clearance rate constant

$$k_{in} = \frac{E_w \cdot G_v}{w\_w} \text{ ; (L } kg^{-1} \text{ } d^{-1}) \quad \textbf{(Eq. S17)}$$

Gill elimination rate constant

$$k_{out} = \frac{k_{in}}{k_{bw}} \text{ ; (kg } kg^{-1} \text{ } d^{-1}) \quad \textbf{(Eq. S18)}$$

Growth dilution rate constant

$$k_G = 0.005 \cdot w\_w^{-0.2} \text{ ; } (d^{-1} \text{ for temperatures around 10°C})$$

$$k_G = 0.00251 \cdot w\_w^{-0.2} \text{ ; } (d^{-1} \text{ for temperatures around 25°C}) \quad \textbf{(Eq. S19)}$$

Chemical internal concentration (excluding metabolism)

$$\frac{dC_{int}(t)}{dt} = \frac{k_{in}}{1000} \cdot C_w(t) - (k_{out} + K_G) \cdot C_{int}(t) \text{ ; } (\mu g\ g^{-1}\ d^{-1}) \quad \textbf{(Eq. S20)}$$

Additional model equation (implementation of whole-body chemical biotransformation)

Metabolite internal concentration

$$\frac{dC_{met}(t)}{dt} = k_{met} \cdot C_{int}(t) \text{ ; } (\mu g\ g^{-1}\ d^{-1}) \quad \textbf{(Eq. S21)}$$

8. Adult multi-compartment physiologically based toxicokinetic (PBTK) model

A multi-compartment PBTK (physiologically based toxicokinetic)[10,11] (Table S4) model was re-developed to predict the abundance of multiple organic chemicals in sub-adult white sturgeon. In addition, the model was adapted to integrate biotransformation by incorporating an *in vivo* intrinsic clearance parameter calculated using an Excel spreadsheet provided by Nichols et al.[7] The *in vivo* intrinsic clearance parameter was used to calculate hepatic clearance, using the well-stirred model of hepatic clearance, which was further used to calculate hepatic biotransformation. A bile compartment was implemented into the existing model structure, by combining hepatic biotransformation with bile volume and bile flow. This component of the model can be used for chemicals that are actively biotransformed and in which values for *in vitro* intrinsic clearance exist. In the present study, *in vitro* intrinsic clearance of B[*a*]P was measured in white sturgeon; however, since no data set pertaining to the bioaccumulation of B[*a*]P exists for any sturgeon species, this parameter could not be tested. Biotransformation was omitted for the simulations using our test chemicals (avermectin-B1,[12.] molinate,[13] sulfamethazine (SM_2),[14] or *p*-nitrophenol (PNP)[15]) as, to our knowledge, no *in vitro* clearance value exists for these chemicals in a sturgeon species.

The model was implemented using Python 3.5® (Python Software Foundation, Wilmington, DE, USA) in Jupyter Notebook® (Project Jupyter, U.S. Patent & Trademark Office, Alexandria, VA, USA). Monte Carlo-like simulations (200 simulations per data point) were run in which a random combination of parameter values from each parameter distribution was chosen, assuming that the parameters are independent. Predictions of the internal concentrations of organic contaminants were generated in the whole body, as well as the liver, fat, richly perfused tissues, and poorly perfused tissues. No predictions for the kidney were generated as, presently, the kidney compartment cannot be accurately parameterized. The model outputs were compared to published data sets of internal concentrations (C_{int}) or muscle concentrations (C_m) for sturgeon that were exposed to the organic contaminants avermectin-

B1,[12] molinate,[13] sulfamethazine (SM_2),[14] or *p*-nitrophenol (PNP).[15] Experimental data sets used for model test and validation purposes are shown in Table S3.

Supplemental Table S3. Experimental data used for modelling internal and muscle chemical concentrations in white sturgeon (*Acipenser transmontanus)* using the PBTK model.

	Chemical	Log K_{OW}[a]	Wet weight	Temp	Exposure Time	Exposure Concentration	Measured C_m	Measured C_{int}
		(-)	(g ± S.D)	(°C)	(h)	(μg L^{-1})	(mg kg^{-1})	(mg kg^{-1})
1	Avermectin B1[b]	4.40	35.8 ± 4.6	20	72	0.2	0.0044	-
2	Avermectin B1[b]	4.40	35.8 ± 4.6	20	120	0.2	0.0066	-
3	Avermectin B1[b]	4.40	35.8 ± 4.6	20	192	0.2	0.0066	-
4	Avermectin B1[b]	4.40	35.8 ± 4.6	20	264	0.2	0.0072	-
5	Avermectin B1[b]	4.40	35.8 ± 4.6	20	336	0.2	0.0074	-
6	Avermectin B1[b]	4.40	35.8 ± 4.6	20	432	0.2	0.0077	-
7	Avermectin B1[b]	4.40	35.8 ± 4.6	20	528	0.2	0.0080	-
8	Avermectin B1[b]	4.40	35.8 ± 4.6	20	24	1	0.0054	-
9	Avermectin B1[b]	4.40	35.8 ± 4.6	20	72	1	0.0198	-
10	Avermectin B1[b]	4.40	35.8 ± 4.6	20	120	1	0.0272	-
11	Avermectin B1[b]	4.40	35.8 ± 4.6	20	192	1	0.0340	-
12	Avermectin B1[b]	4.40	35.8 ± 4.6	20	264	1	0.0364	-
13	Avermectin B1[b]	4.40	35.8 ± 4.6	20	336	1	0.0364	-
14	Avermectin B1[b]	4.40	35.8 ± 4.6	20	432	1	0.0383	-
15	Avermectin B1[b]	4.40	35.8 ± 4.6	20	528	1	0.0383	-
16	Molinate[c]	3.21	15.6 ± 1.9	18	50 + 24 depuration	100	-	2.748
17	Sulfamethazine[d]	0.53	28.2 ± 5.1	20	6	100	0.10	-
18	Sulfamethazine[d]	0.53	28.2 ± 5.1	20	12	100	0.097	-
19	Sulfamethazine[d]	0.53	28.2 ± 5.1	20	24	100	0.099	-
20	Sulfamethazine[d]	0.53	28.2 ± 5.1	20	48	100	0.102	-
21	Sulfamethazine[d]	0.53	28.2 ± 5.1	20	72	100	0.100	-
22	Sulfamethazine[d]	0.53	28.2 ± 5.1	20	96	100	0.097	-
23	Sulfamethazine[d]	0.53	28.2 ± 5.1	20	120	100	0.098	-
24	Sulfamethazine[d]	0.53	28.2 ± 5.1	20	144	100	0.097	-

25	Sulfamethazine[d]	0.53	28.2 ± 5.1	20	192	1000	0.097	-
26	Sulfamethazine[d]	0.53	28.2 ± 5.1	20	6	1000	0.094	-
27	Sulfamethazine[d]	0.53	28.2 ± 5.1	20	12	1000	0.479	-
28	Sulfamethazine[d]	0.53	28.2 ± 5.1	20	24	1000	0.574	-
29	Sulfamethazine[d]	0.53	28.2 ± 5.1	20	48	1000	0.747	-
30	Sulfamethazine[d]	0.53	28.2 ± 5.1	20	72	1000	0.795	-
31	Sulfamethazine[d]	0.53	28.2 ± 5.1	20	96	1000	0.779	-
32	Sulfamethazine[d]	0.53	28.2 ± 5.1	20	120	1000	0.811	-
33	Sulfamethazine[d]	0.53	28.2 ± 5.1	20	144	1000	0.795	-
34	Sulfamethazine[d]	0.53	28.2 ± 5.1	20	192	1000	0.820	-
35	p-nitrophenol[e]	1.91	9.9 ± 0.3	17	3	1000	-	8.350
36	p-nitrophenol[e]	1.91	9.9 ± 0.3	17	7	1000	-	12.700
37	p-nitrophenol[e]	1.91	9.9 ± 0.3	17	24	1000	-	15.020
38	p-nitrophenol[e]	1.91	9.9 ± 0.3	17	24	1000	-	15.816
39	p-nitrophenol[e]	1.91	9.9 ± 0.3	17	24 + 24 depuration	1000	-	1.680

a value obtained from PubChem® (U.S. National Library of Medicine)
b Shen et al.[12]
c Tjeerdema & Crosby[13]
d Hou et al.[14]
e Tenbrook et al.[15]

Supplemental Table S4. Model inputs and parameters of the multi-compartment PBTK model for sub-adult white sturgeon (*Acipenser transmontanus*). The table is based on Stadnicka et al.[10]. Compartment volumes were expressed relative to the total body volume, while all compartments were assumed to have a specific gravity of 1.0 (i.e., the units L and kg can be substitute for another).

Symbol	Units	Description	Value
w_w	kg (L)	Body wet mass (volume of the whole body)	– Model input – (0.622)
log K_{ow}	-	Octanol-water partitioning coefficient	– Model input –
C_w	µg L^{-1}	Chemical concentration in inspired water	– Model input –
T	°C	Water temperature	– Model input –
C_{ox}	mg L^{-1}	Dissolved oxygen concentration in inspired water	– Model input –
lipid	-	Total lipid content (fraction of body weight)	– Model input – (0.1)
K	-	Constant in equation S23, for T>10°C	$3.05\ 10^{-4}$ [a]
n	-	Constant in equation S23, for T>10°C	1.855[a]
m	-	Constant in equation S23, for T>10°C	-0.138[a]
α_b	-	Lipid content of blood tissue (fraction of wet weight)	0.008
α_f	-	Lipid content of fat tissue (fraction of wet weight)	– calculated –
α_k	-	Lipid content of kidney tissue (fraction of wet weight)	0.008
α_l	-	Lipid content of liver tissue (fraction of wet weight)	0.306
α_m	-	Lipid content of muscle tissue (fraction of wet weight)	0.0262
γ_b	-	Water content of blood tissue (fraction of wet weight)	0.866
γ_f	-	Water content of fat tissue (fraction of wet weight)	0.342
γ_k	-	Water content of kidney tissue (fraction of wet weight)	0.875

γ_l	-	Water content of liver tissue (fraction of wet weight)	0.510
γ_m	-	Water content of muscle tissue (fraction of wet weight)	0.763
$lipid_l$	-	Lipid content of lean tissue (fraction of wet weight)	– Equation S22 –
V_f	L	Volume of the fat compartment	– Equation S23 –
V_l	L	Volume of the liver compartment	0.029 w_w
V_m	L	Volume of the poorly perfused compartment	– Equation S24 –
V_r	L	Volume of the richly perfused compartment	0.058 w_w
Q_c	L h^{-1}	Cardiac output	– Equation S25 –
Q_f	L h^{-1}	Blood flow to the fat compartment	0.010 Q_c (assumued)
Q_l	L h^{-1}	Blood flow to the liver compartment	0.071 Q_c
Q_m	L h^{-1}	Blood flow to the poorly perfused compartment	0.717 Q_c
Q_r	L h^{-1}	Blood flow to the richly perfused compartment	0.202 Q_c
VO_2	mg h^{-1}	Oxygen consumption rate normalized to 1 kg body weight	– Equation S26 –
Q_w	L h^{-1}	Effective respiratory volume	– Equation S27 –
P_{bw}	-	Blood:water partitioning coefficient	– Equation S28 –
P_l,P_f,P_m	-	Liver/fat/muscle:blood partitioning coefficient	– Equation S29 –
P_r	-	Richly perfused tissue:blood partitioning coefficient	– P_l –
A_i	µg	Chemical amount in fat, poorly and richly perfused tissues	– Equation S30 –
A_l	µg	Chemical amount in the liver compartment	– Equation S31 –
A_l_transform	µg	Hepatic biotransformation	– Equation S35 –
A_{bile}	µg	Chemical amount in bile compartment	– Equation S36 –
$CL_{int,\ in\ vivo}$	L d^{-1} kg^{-1}	*In vivo* intrinsic clearance	– Equation S3 –

Cl_H	L d^{-1} kg^{-1}	Hepatic clearance	– Equation S5 –
C_{int}	µg g^{-1}	Internal concentration in the whole fish	– Equation S32 –
C_{art}	µg L^{-1}	Chemical concentration in arterial blood	– Equation S33 –
C_{ven}	µg L^{-1}	Chemical concentration in venous blood	– Equation S34 –
C_{bile}	µg L^{-1}	Metabolite concentration in bile	– Equation S37 –

Multi-compartment PBTK model equations (from Stadnicka et al.[10])

Volume of the lean tissue compartment

$$lipid_l = \frac{V_l \cdot \alpha_l + V_r \cdot \alpha_r + V_m \cdot \alpha_m + V_k \cdot a_k}{V_l + V_r + V_m + V_k}$$; (unitless)

(Eq. S22)

Volume of the fat compartment

$$V_f = w\_w \cdot \frac{lipid - lipid_l}{\alpha_f - lipid_l}$$; (L) **(Eq. S23)**

Volume of the poorly perfused compartment

$$V_m = w\_w - (V_l + V_r + V_k + V_f)$$; (L) **(Eq. S24)**

Cardiac output

$$Q_c = (0.23 \cdot T - 0.78) \cdot \left(\frac{1000 \cdot w\_w}{500}\right)^{-0.1} \cdot w\_w^{0.75}$$; (L h^{-1}) **(Eq. S25)**

Oxygen consumption rate

$$VO_2 = K \cdot (32 + T \cdot \frac{9}{5})^n \cdot \left(\frac{w\_w}{0.4536}\right)^m \cdot \frac{10000}{24}$$; (mg h^{-1}) **(Eq. S26)**

Effective respiratory volume

$$Q_w = \frac{VO_2}{0.8 \cdot C_{ox}} \cdot w\_w^{0.75}$$; (L h^{-1}) **(Eq. S27)**

Blood:water partitioning coefficient

$$P_{bw} = 10^{0.72 \cdot \log Kow + 1.04 \cdot log(\alpha_b) + 0.86} + \gamma_b$$; (unitless) **(Eq. S28)**

Liver/fat/muscle:blood partitioning coefficient

$$P_{l,f,m} = \frac{10^{0.72 \cdot \log Kow + 1.04 \cdot log(\alpha_{l,f,m}) + 0.86} + \gamma_{l,f,m}}{P_{bw}}$$; (unitless) **(Eq. S39)**

Chemical amount in fat, poorly and richly perfused tissues

$$\frac{dA_i(t)}{dt} = Q_i \cdot \left(C_{art}(t) - \frac{A_i(t)}{V_i \cdot P_i}\right)$$; (µg h^{-1}) **(Eq. S30)**

Chemical amount in the liver compartment

$$\frac{dA_l(t)}{dt} = Q_r \cdot \frac{A_r(t)}{V_r \cdot P_r} + Q_l \cdot C_{art}(t) - (Q_r + Q_l) \cdot \frac{A_l(t)}{V_l \cdot P_l} - A_{l\_transform}(t) \text{ ; (µg h}^{-1}\text{)} \quad \textbf{(Eq. S31)}$$

Internal chemical concentration in the whole fish

$$C_{int}(t) = \frac{A_f(t) + A_m(t) + A_r(t) + A_l(t) + A_k(t)}{1000 \cdot w\_w} \text{ ; (µg g}^{-1}\text{)} \quad \textbf{(Eq. S32)}$$

Chemical concentration in arterial blood

$$C_{art}(t) = \min\left(Q_w, Q_c \cdot P_{bw}\right) \cdot C_w - \frac{C_{ven}(t)}{P_{bw}} \cdot \frac{1}{Q_c} + C_{ven}(t) \text{ ; (µg L}^{-1}\text{)} \quad \textbf{(Eq. S33)}$$

Chemical concentration in venous blood $C_{ven}(t) =$

$$\frac{Q_f \cdot \frac{A_f(t)}{V_f \cdot P_f} + 0.4 \cdot Q_m \cdot \frac{A_m(t)}{V_m \cdot P_m} + (0.6 \cdot Q_m + Q_k) \cdot \frac{A_k(t)}{V_k \cdot P_k} + (Q_r + Q_l) \cdot \frac{A_l(t)}{V_l \cdot P_l}}{Q_c} \text{ ; (µg L}^{-1}\text{)} \quad \textbf{(Eq. S34)}$$

Additional model equations (implementation of chemical biotransformation and bile compartment)

Hepatic biotransformation

$$\frac{dA_{l\_transform}(t)}{dt} = Cl_H \cdot \frac{A_l}{V_l \cdot P_l} \text{ ; (µg h}^{-1}\text{)} \quad \textbf{(Eq. 35)}$$

Chemical amount in the bile

$$A_{bile} = A_{bile} - A_{bile} \cdot \frac{Q_{bile}}{V_{bile}} \text{ ; (µg h}^{-1}\text{)} \quad \textbf{(Eq.36)}$$

Metabolite concentration in bile

$$C_{bile}(t) = \frac{A_{bile}}{V_{bile}} \text{ ; (µg L}^{-1}\text{)} \quad \textbf{(Eq.37)}$$

9. Results

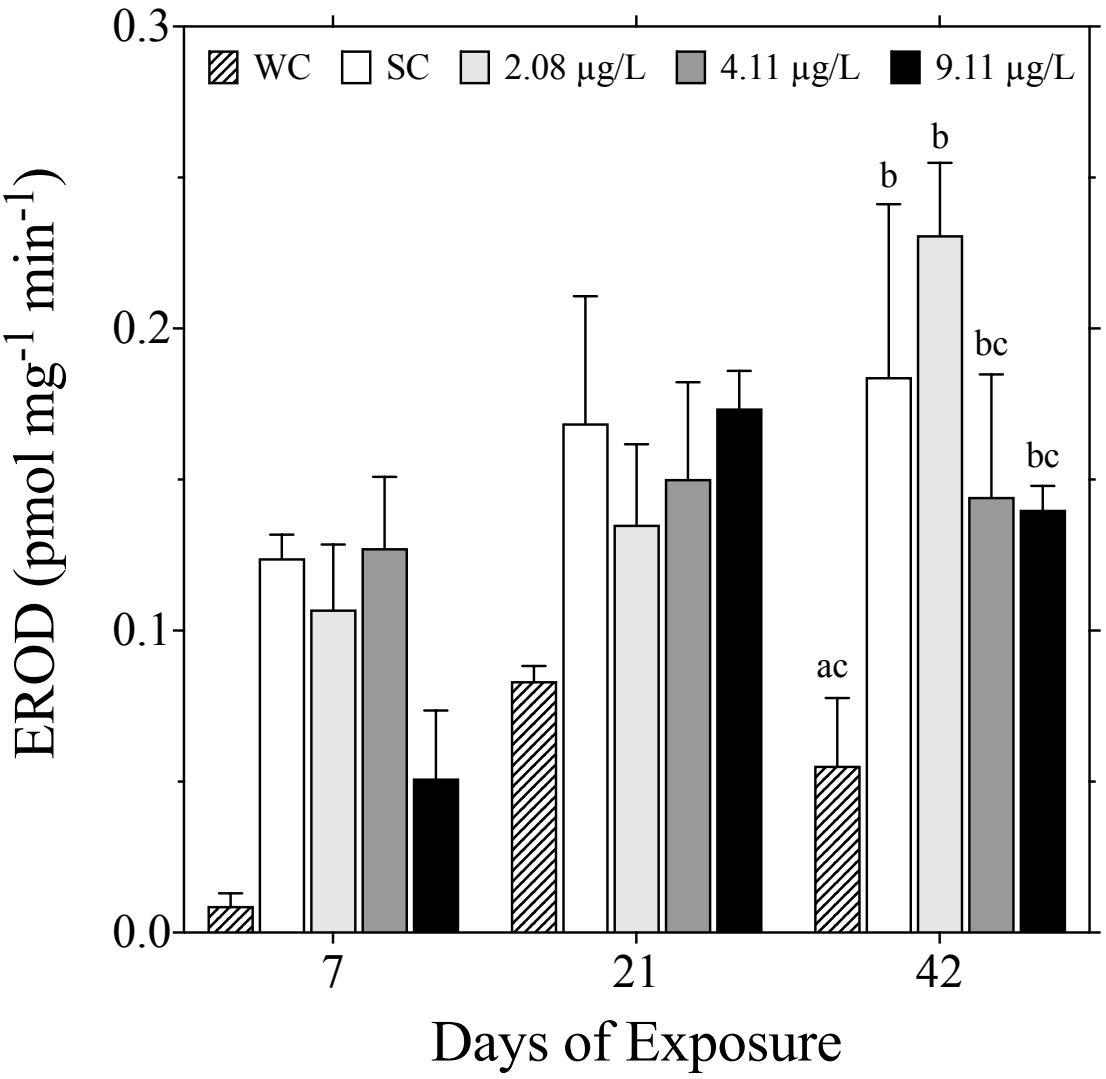

Figure S2. EROD activity (pmol mg^{-1} min^{-1}) for whole-body embryo-larval white sturgeon after seven, 21, and 42 days of exposure to increasing concentrations of B[*a*]P as well as water control (WC) and solvent control (SC), respectively. Data are expressed as mean ± SEM. Different letters denote a significant difference in EROD activity among treatment groups within each respective time point (2-way ANOVA, $\alpha = 0.05$). No differences existed among treatment groups on day 12 or 21 of exposure.

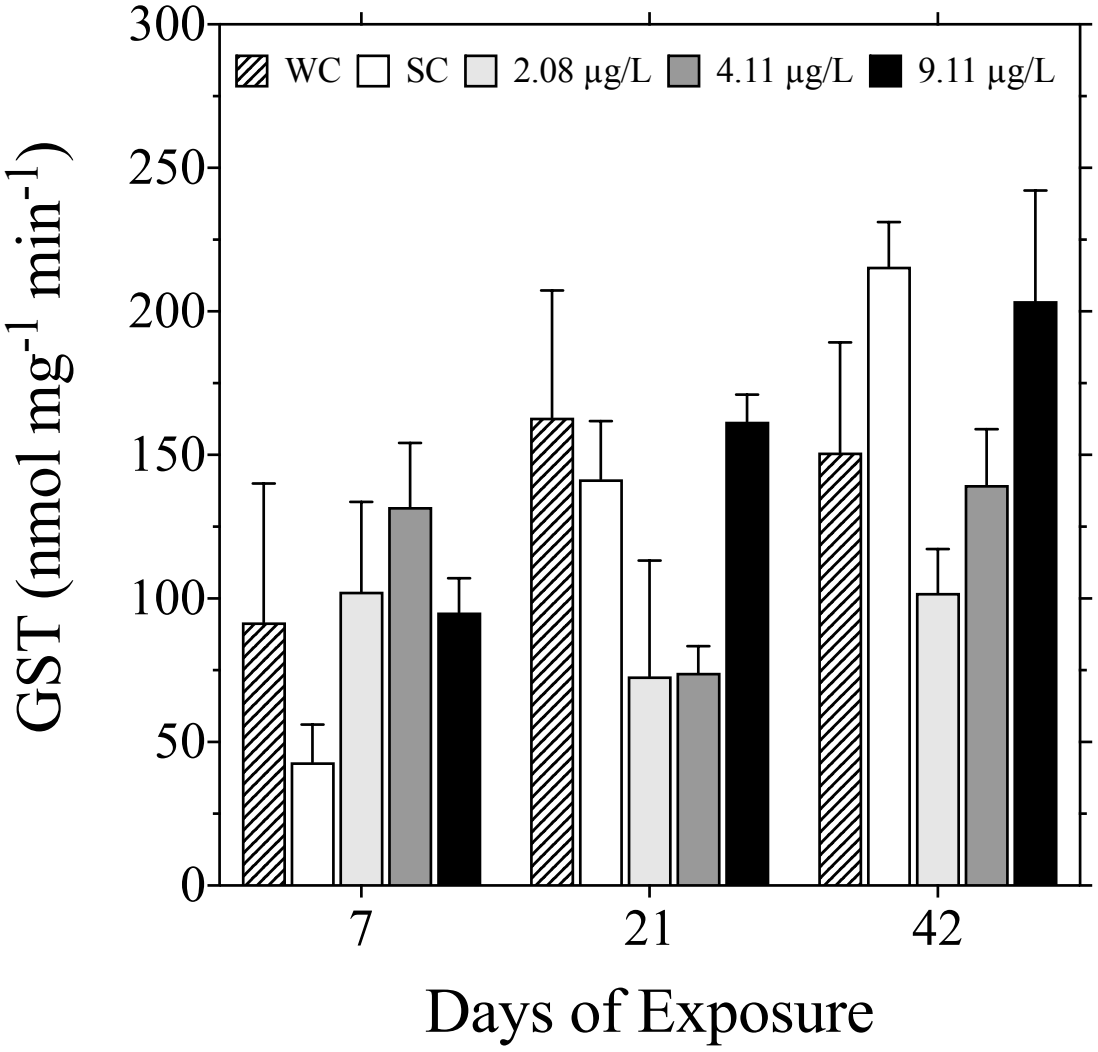

Figure S3. GST activity (nmol mg^{-1} min^{-1}) for whole-body embryo-larval white sturgeon after seven, 21, and 42 days of exposure to increasing concentrations of B[*a*]P as well as water control (WC) and solvent control (SC), respectively. Data are expressed as mean ± SEM. No differences existed among treatment groups within each respective time point (2-way ANOVA, $\alpha = 0.05$).

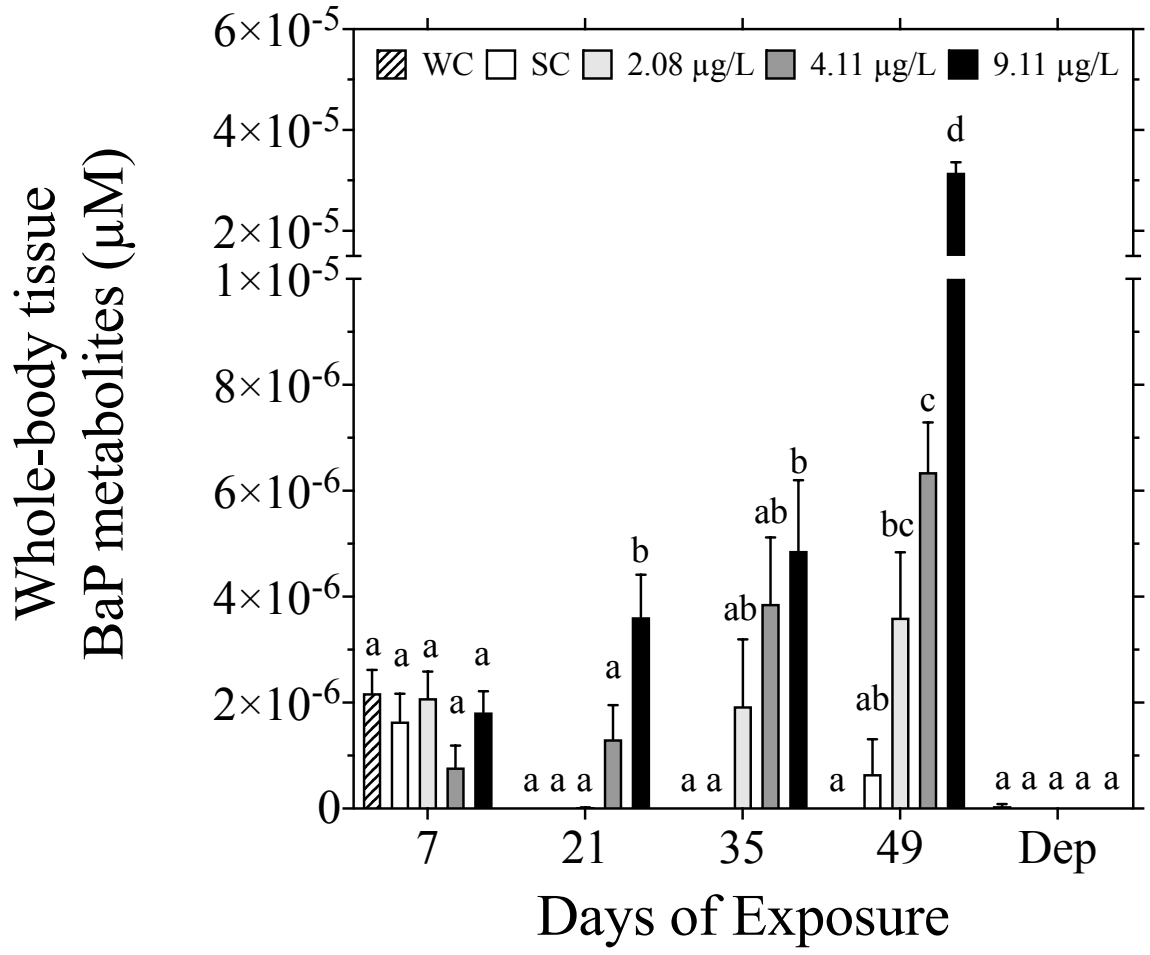

Figure S4. Abundance of B[*a*]P metabolites (µM) in whole-body embryo-larval white sturgeon after seven, 12, 21, 35 and 49 days of exposure to increasing concentrations of B[*a*]P as well as water control (WC) and solvent control (SC). Data are expressed as mean ± SEM. Different letters denote a significant difference in B[*a*]P metabolites between treatment groups within each respective time point (One-way ANOVA with Tukey's HSD, $\alpha = 0.05$).

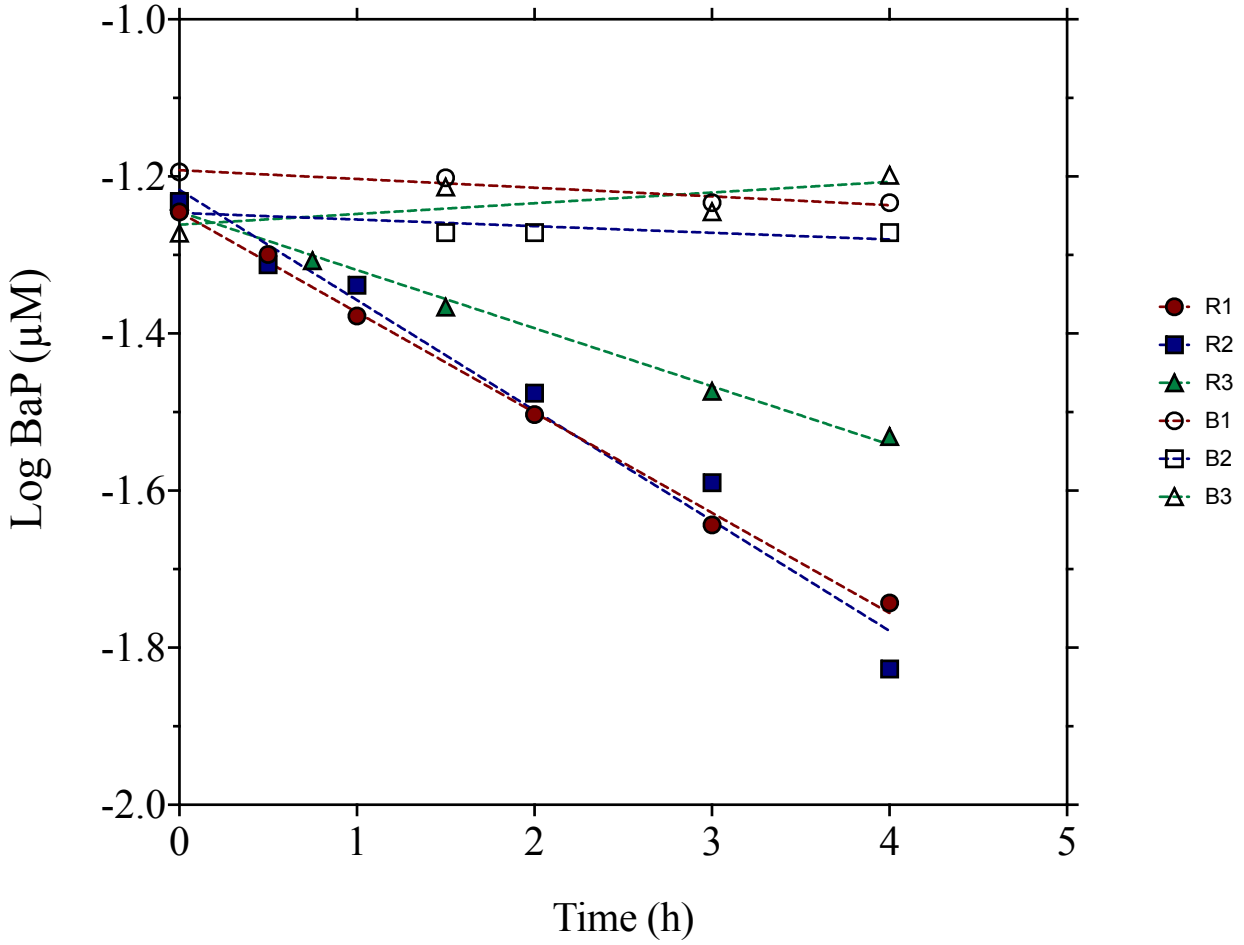

Figure S5. Substrate depletion curves from the sub-adult white sturgeon *in-vitro* clearance assay (SI Section 5). R = replicate; B = blank; BaP = benzo[*a*]pyrene; µM = microMolar; h = hours.

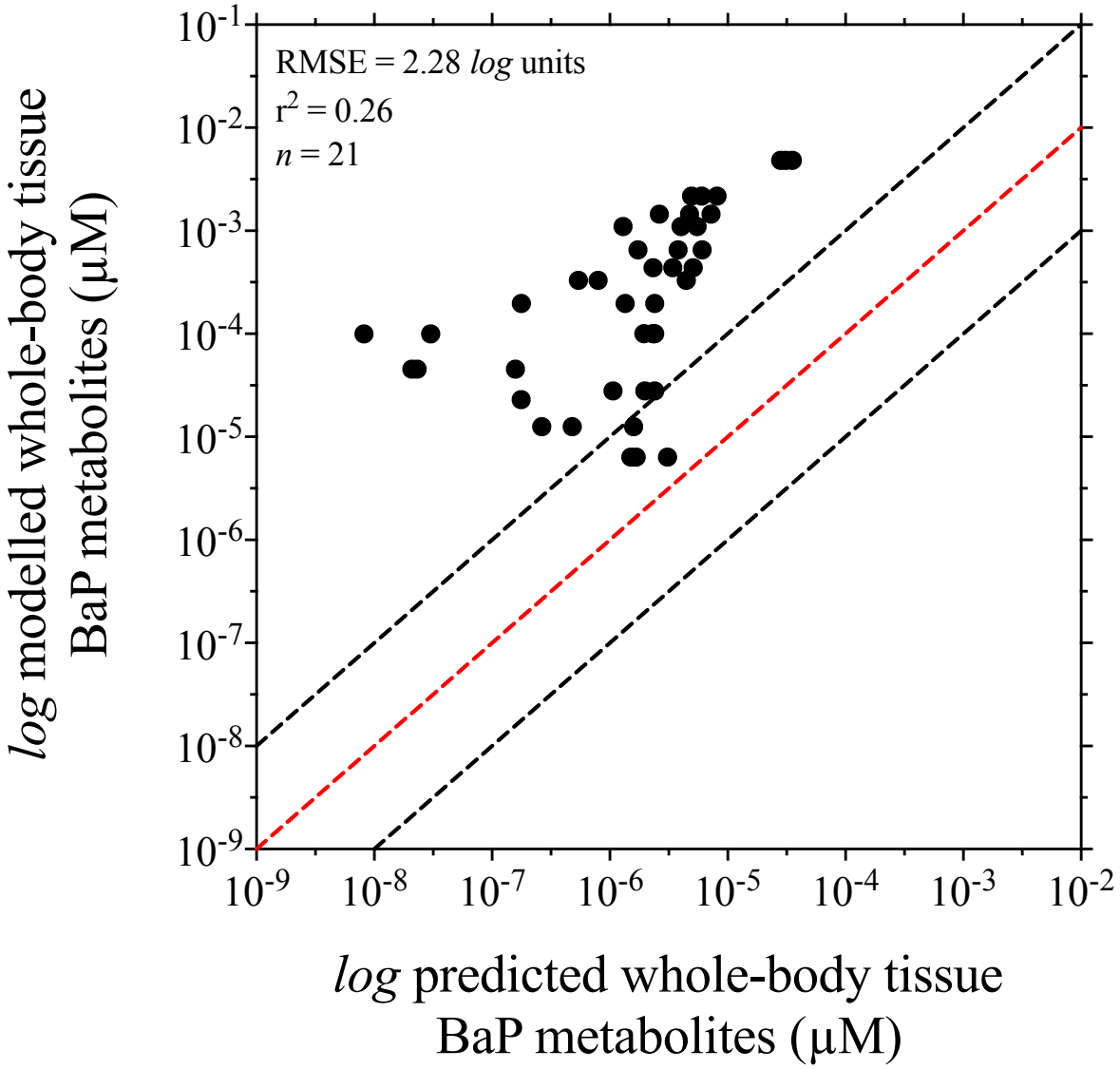

Figure S6. Model predictions of embryo-larval whole-body biotransformation in the white sturgeon when k_{MET} is scaled using the value for sub-adult *in vitro* clearance (0.219 mL h^{-1} mg^{-1}). The figure shows the relationship between predicted and measured concentrations of whole-body tissue B[*a*]P metabolites generated from the calibrated values of whole-body biotransformation. The dashed red line represents the equality line, and the dashed black lines represent the ± 10-fold deviation from equality. The parameter was determined using a training set of 21 data points and adjusted until the highest achievable number of predictions were within 1-order of magnitude from the measured values. RMSE, root mean squared error.

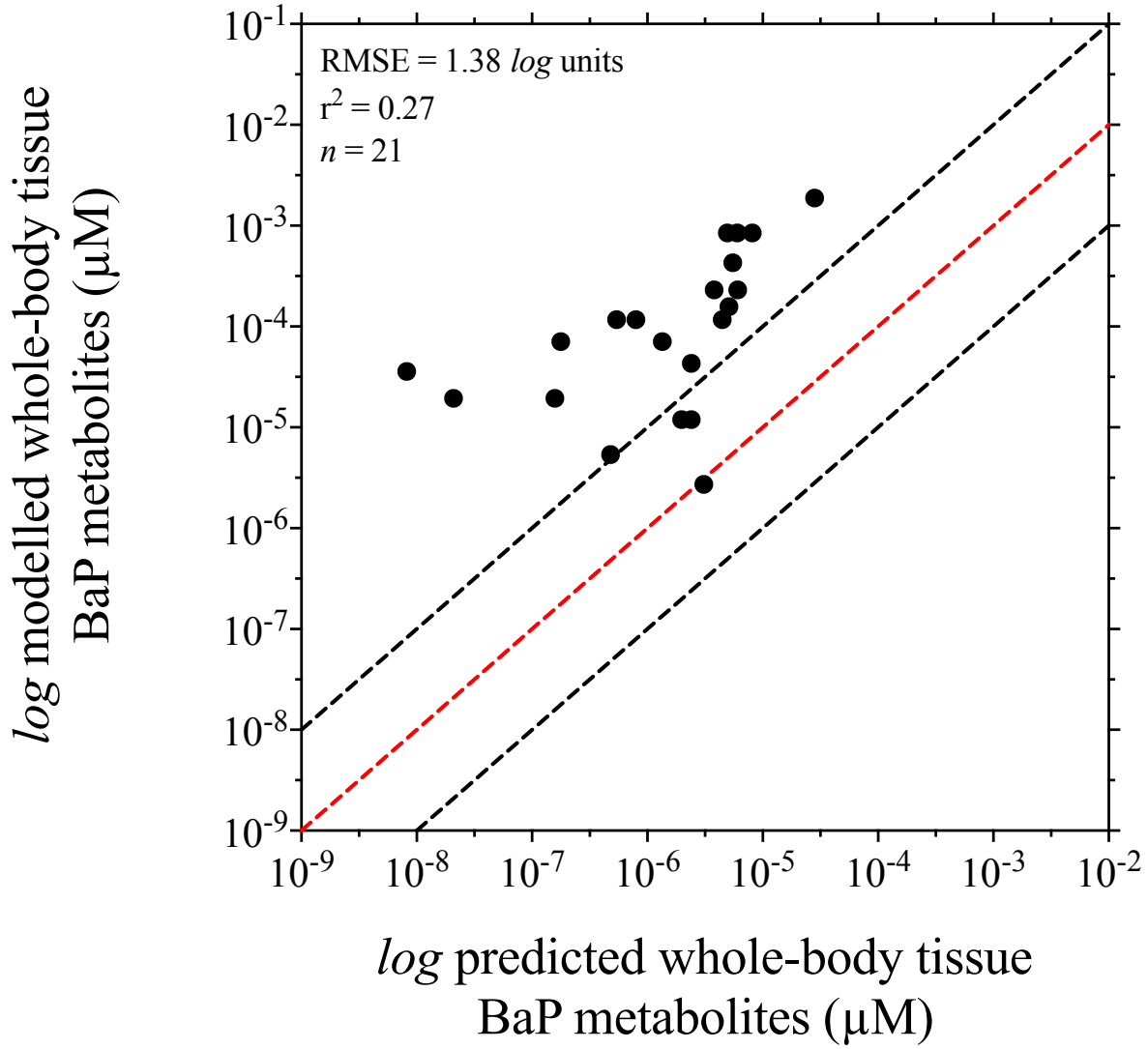

Figure S7. Calibration of embryo-larval whole-body biotransformation in the white sturgeon when k_{MET} using an *in vitro* clearance value of 0.05 mL h^{-1} mL^{-1} (i.e., the LOD from OECD 319B[2]). The figure shows the relationship between predicted and measured concentrations of whole-body tissue B[*a*]P metabolites generated from the calibrated values of whole-body biotransformation. The dashed red line represents the equality line, and the dashed black lines represent the ± 10-fold deviation from equality. The parameter was determined using a training set of 21 data points and adjusted until the highest achievable number of predictions were within 1-order of magnitude from the measured values. RMSE, root mean squared error.

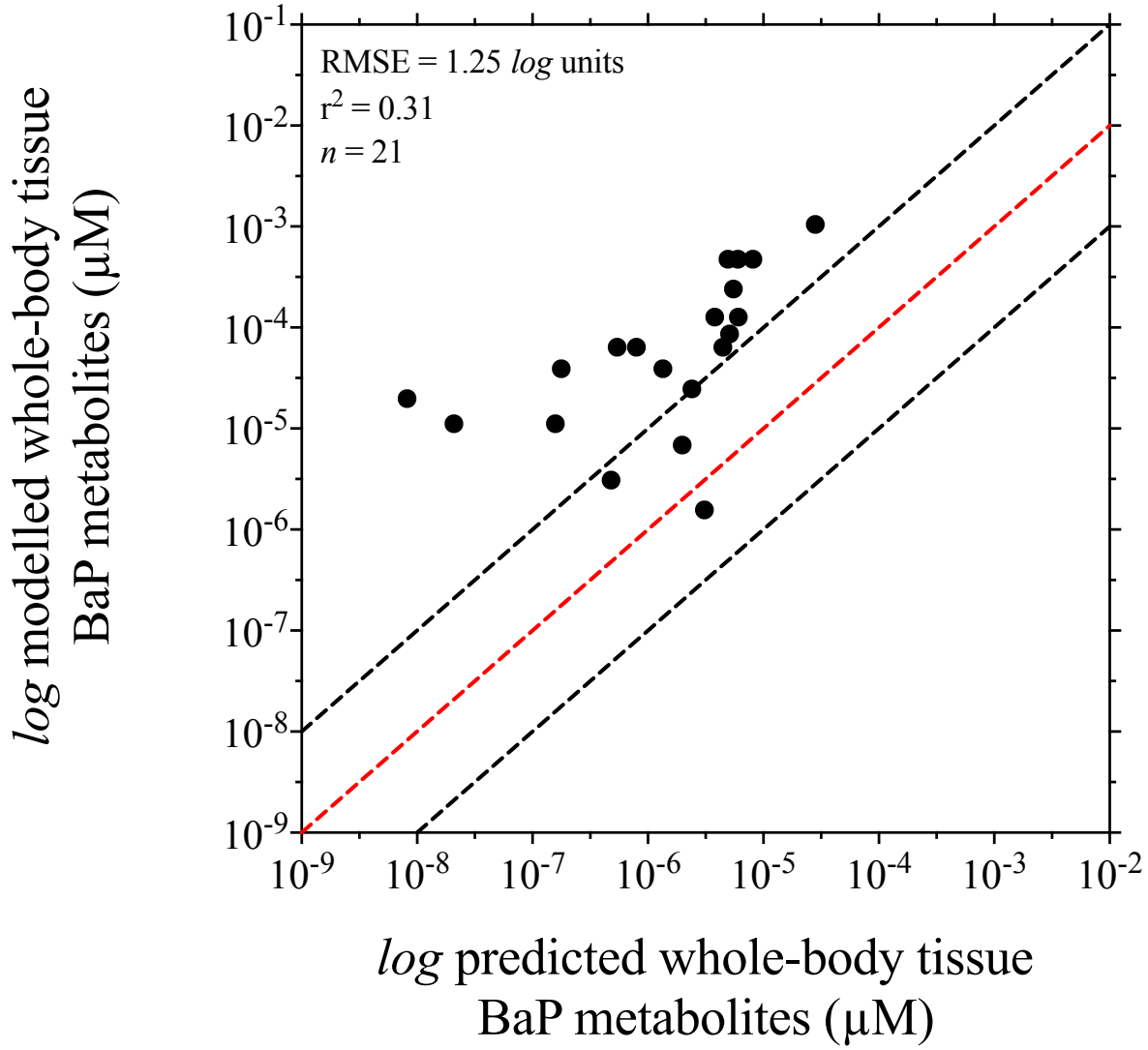

Figure S8. Calibration of embryo-larval whole-body biotransformation in the white sturgeon when k_{MET} using an *in vitro* clearance value of 0.025 mL h^{-1} mL^{-1} (i.e., half the LOD from OECD 319B[2]). The figure shows the relationship between predicted and measured concentrations of whole-body tissue B[*a*]P metabolites generated from the calibrated values of whole-body biotransformation. The dashed red line represents the equality line, and the dashed black lines represent the ± 10-fold deviation from equality. The parameter was determined using a training set of 21 data points and adjusted until the highest achievable number of predictions were within 1-order of magnitude from the measured values. RMSE, root mean squared error.

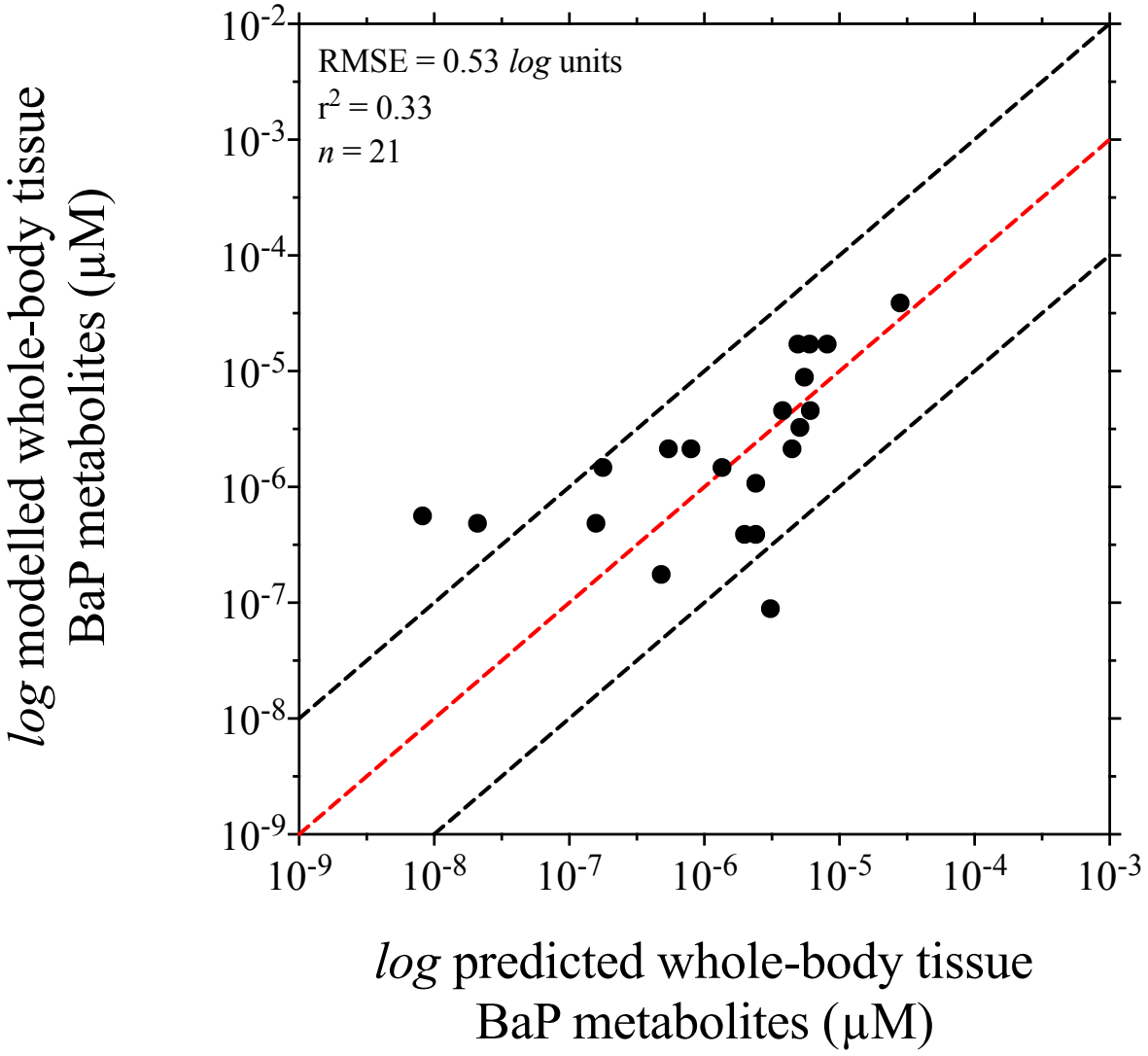

Figure S9. Calibration of embryo-larval whole-body biotransformation in the white sturgeon when k_{MET} using an *in vitro* clearance value of 0.00078 mL h^{-1} mL^{-1}. The figure shows the relationship between predicted and measured concentrations of whole-body tissue B[*a*]P metabolites generated from the calibrated values of whole-body biotransformation. The dashed red line represents the equality line, and the dashed black lines represent the ± 10-fold deviation from equality. The parameter was determined using a training set of 21 data points and adjusted until the highest achievable number of predictions were within 1-order of magnitude from the measured values. RMSE, root mean squared error.

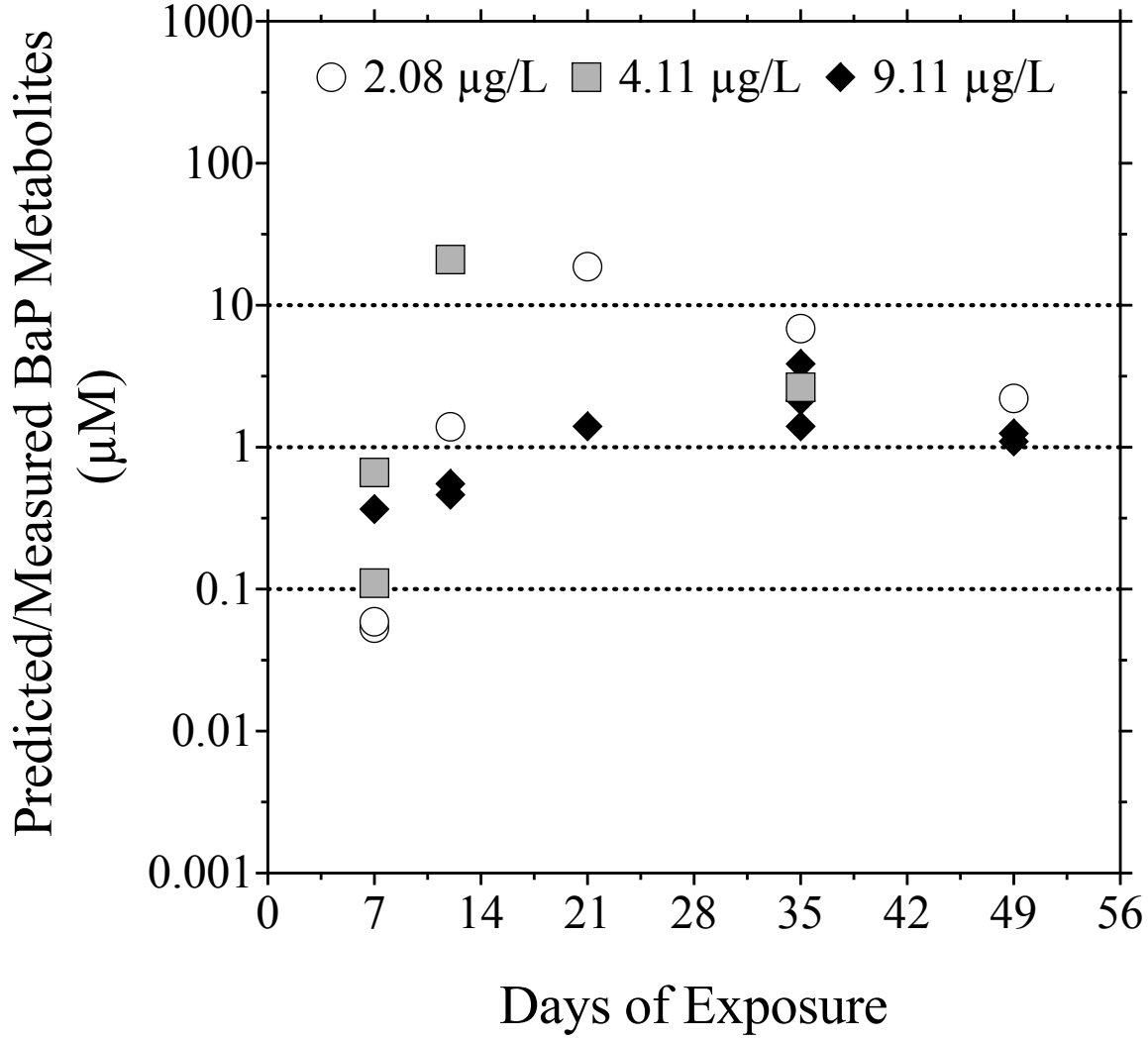

Figure S10. Relationships between predicted and measured concentrations of whole-body tissue B[*a*]P from the white sturgeon embryo-larval one compartment model relative to the day of exposure with ± 10-fold error from equality (grey). Predicted whole-body tissue B[*a*]P concentrations were obtained directly from model outputs.

12. References

1. Kennedy, S. W., & Jones, S. P. Simultaneous measurement of cytochrome P4501A catalytic activity and total protein concentration with a fluorescence plate reader. *Anal. Biochem.* **1994**, *222*(1), 217-223. DOI 10.1006/abio.1994.1476.

2.OECD. Test No. 319B: Determination of in vitro intrinsic clearance using rainbow trout liver S9 sub-cellular fraction (RT-S9). *OECD Guidelines for the Testing of Chemicals* **2018**, Section 3, OECD Publishing, Paris, DOI 10.1787/9789264303232-en.

3. Habig, W. H., Pabst, M. J., & Jakoby, W. B. (1974). Glutathione S-transferases the first enzymatic step in mercapturic acid formation. *Journal of biological Chemistry*, *249*(22), 7130-7139.

4. Richardson, S.J, Bai, A., A Kulkarni, A., & F Moghaddam, M. Efficiency in drug discovery: liver S9 fraction assay as a screen for metabolic stability. *Drug Metab. Lett.* ***2016***, *10*(2), 83-90. DOI 10.2174/1872312810666160223121836

5. Lu, Y., Ludsin, S. A., Fanslow, D. L., & Pothoven, S. A. Comparison of three microquantity techniques for measuring total lipids in fish. *Can. J. Fish. Aquat. Sci.* **2008**, *65*(10), 2233-2241. DOI 10.1139/F08-135.

6. Arnot, J. A., & Gobas, F. A. A food web bioaccumulation model for organic chemicals in aquatic ecosystems. *Environ. Tox. Chem.* **2004**, *23* (10), 2343-2355; DOI 10.1897/03-438.

7. Nichols, J. W., Fitzsimmons, P. N., & Burkhard, L. P. In vitro-in vivo extrapolation of quantitative hepatic biotransformation data for fish. II. Modeled effects on chemical bioaccumulation. *Environ. Tox. Chem.* **2007**, 26(6), 1304–1319. DOI 10.1897/06-259r.1.

8. Grimard, C., Mangold-Döring, A., Schmitz, M., Alharbi, H., Jones, P. D., Giesy, J. P., Hecker, M., & Brinkmann, M. . *In vitro-in vivo* and cross-life stage extrapolation of uptake and biotransformation of benzo[*a*]pyrene in the fathead minnow (*Pimephales promelas*). *Aquat. Toxicol.* **2020.** 105616. DOI 10.1016/j.aquatox.2020.105616.

9. Debruyn, A. M., & Gobas, F. A. The sorptive capacity of animal protein. *Environ. Toxicol. Chem.* 2007, *26*(9), 1803-1808. DOI 0.1897/07-016R.1

10. Stadnicka, J., Schirmer, K., & Ashauer, R. (2012). Predicting concentrations of organic chemicals in fish by using toxicokinetic models. *Environ. Sci. Tech.* **2012**, 46(6), 3273–3280. DOI 10.1021/es2043728.

11. Brinkmann, M., Schlechtriem, C., Reininghaus, M., Eichbaum, K., Buchinger, S., Reifferscheid, G., ... & Preuss, T. G. Cross-species extrapolation of uptake and disposition of neutral organic chemicals in fish using a multispecies physiologically-based toxicokinetic model framework. *Environ Sci. Technol.* **2016**, 50(4), 1914-1923. DOI 10.1021/acs.est.5b06158.

12. Shen, J., Zhang, Q., Ding, S., Zhang, S., & Coats, J. R. Bioconcentration and elimination of avermectin B1 in sturgeon. *Environ. Tox. Chem.* ***2005***, *24*(2), 396-399. DOI 10.1897/03-480.1.

13. Tjeerdema, R. S., & Crosby, D. G. Comparative biotransformation of molinate (Ordram®) in the white sturgeon (Acipenser transmontanus) and common carp (Cyprinus carpio). *Xenobiotica* **1988**, *18*(7), 831-838. DOI 10.3109/00498258809041721.

14. Hou, X., Shen, J., Zhang, S., Jiang, H., & Coats, J. R. Bioconcentration and elimination of sulfamethazine and its main metabolite in sturgeon (Acipenser schrenkii). *J. Agric. Food Chem.* **2003**, *51*(26), 7725-7729. DOI 10.1021/jf030492+.

15. TenBrook, P. L., Kendall, S. M., & Tjeerdema, R. S. Toxicokinetics and biotransformation of p-nitrophenol in white sturgeon (Acipenser transmontanus). *Ecotoxicol. Environ. Saf.* **2006**, *64*(3), 362-368. DOI 10.1016/j.ecoenv.2005.04.006.